

Review

Open Access



# Recent progress of molybdenum-based nitrides/carbides catalysts for lithium-sulfur batteries

Qiyuan Fan<sup>1,4</sup>, Hao Song<sup>1</sup>, Biao Gao<sup>1</sup>, Lei Wang<sup>2,\*</sup>, Paul K. Chu<sup>3,\*</sup>, Kaifu Huo<sup>4,\*</sup>

<sup>1</sup>State Key Laboratory of Advanced Refractories and Metallurgy and Institute of Advanced Materials and Nanotechnology, Wuhan University of Science and Technology, Wuhan 430081, Hubei, China.

<sup>2</sup>State Key Laboratory of Advanced Papermaking and Paper-based Materials, South China University of Technology, Guangzhou 510641, Guangdong, China.

<sup>3</sup>Department of Physics, Department of Materials Science and Engineering, and Department of Biomedical Engineering, City University of Hong Kong, Kowloon, Hong Kong 999077, China.

<sup>4</sup>Wuhan National Laboratory for Optoelectronics (WNLO), Huazhong University of Science and Technology, Wuhan 430074, Hubei, China.

**\*Correspondence to:** Dr. Lei Wang, State Key Laboratory of Advanced Papermaking and Paper-based Materials, South China University of Technology, Guangzhou 510641, Guangdong, China. E-mail: felwang@scut.edu.cn; Prof. Paul K. Chu, Department of Physics, Department of Materials Science and Engineering, and Department of Biomedical Engineering, City University of Hong Kong, 83 Tat Chee Avenue, Kowloon Tong, Hong Kong 999077, China. E-mail: paul.chu@city.edu.hk; Prof. Kaifu Huo, Wuhan National Laboratory for Optoelectronics (WNLO), Huazhong University of Science and Technology, 1037 Luoyu Road, Hongshan District, Wuhan 430074, Hubei, China. E-mail: kfhuo@hust.edu.cn

**How to cite this article:** Fan, Q.; Song, H.; Gao, B.; Wang, L.; Chu, P. K.; Huo, K. Recent progress of molybdenum-based nitrides/carbides catalysts for lithium-sulfur batteries. *Energy Mater.* 2025, 5, 500105. <https://dx.doi.org/10.20517/energymater.2025.33>

**Received:** 10 Feb 2025 **First Decision:** 3 Mar 2025 **Revised:** 23 Mar 2025 **Accepted:** 8 Apr 2025 **Published:** 16 May 2025

**Academic Editors:** Jung Ho Kim, Jiaqi Huang **Copy Editor:** Fangling Lan **Production Editor:** Fangling Lan

## Abstract

Lithium-sulfur (Li-S) batteries stand out due to their high theoretical energy density, natural abundance of sulfur, and cost-effectiveness. Despite these advantages, challenges such as the shuttle effect of lithium polysulfides, electrode degradation, and safety concerns hinder their commercialization. Recent advances have focused on integrating molybdenum-based nitrides and carbides to address these issues. These materials offer advantages such as tunable compositions, adjustable lattice structures, semi-metallic conductivity, and enhanced catalytic activity and electron transport. In this mini-review, we delve into the unique physicochemical properties of molybdenum-based nitrides and carbides and the associated composites and their roles in improving the properties of Li-S batteries and discuss their applications as sulfur cathodes and interlayers, mechanisms of lithium polysulfides adsorption, and effects on reaction kinetics. This review aims to consolidate existing knowledge,



© The Author(s) 2025. **Open Access** This article is licensed under a Creative Commons Attribution 4.0 International License (<https://creativecommons.org/licenses/by/4.0/>), which permits unrestricted use, sharing, adaptation, distribution and reproduction in any medium or format, for any purpose, even commercially, as long as you give appropriate credit to the original author(s) and the source, provide a link to the Creative Commons license, and indicate if changes were made.



identify research gaps, and inspire future advancements in Li-S battery technology, paving the way for high-performance, sustainable energy storage solutions.

**Keywords:** Lithium-sulfur battery, polysulfide conversion, catalytic activity, molybdenum carbide, molybdenum nitride

## INTRODUCTION

The global market for energy storage systems (ESSs) has undergone rapid expansion over the past few decades. However, current ESSs are struggling to meet the growing demand for grid-connected storage solutions<sup>[1-4]</sup>. As a result, there is an urgent need for batteries to offer higher energy and power densities in addition to reduced production costs<sup>[5]</sup>. Among the various battery designs, lithium-sulfur (Li-S) batteries constitute a promising option due to their high theoretical energy density of 2,600 Wh kg<sup>-1</sup>, which is more than five times that of traditional Li-ion batteries. Additionally, the sulfur cathode provides advantages such as natural abundance, environmental friendliness, and cost-effectiveness<sup>[6-8]</sup>.

The commonly accepted reaction mechanism in Li-S batteries involves the transfer of multiple electrons<sup>[9,10]</sup>, characterized by a series of sulfur-species reactions and the formation of soluble multiple intermediates during charging and discharging cycles [Figure 1A]<sup>[11]</sup>. During lithiation, sulfur (density: 2.36 g cm<sup>-3</sup>) is converted into Li<sub>2</sub>S (density: 1.67 g cm<sup>-3</sup>), and the significant volume expansion of approximately 80% leads to electrode degradation and pulverization. Moreover, the insulating properties of sulfur and its discharge products, Li<sub>2</sub>S<sub>2</sub> and Li<sub>2</sub>S, hinder electron transfer and reaction kinetics<sup>[12,13]</sup>. In contrast to Li<sub>2</sub>S<sub>2</sub> and Li<sub>2</sub>S, soluble lithium polysulfides (LiPSs) can permeate through the porous separator and react with the lithium metal anode to form insoluble Li<sub>2</sub>S. This phenomenon, known as the "shuttle effect", depletes the sulfur cathode and passivates the lithium metal anode, resulting in increased internal resistance, reduced cycling stability, and lower Coulombic efficiency. Furthermore, the lithium metal anode is plagued by high chemical reactivity, an unstable solid electrolyte interphase (SEI), and the formation of lithium dendrites during the plating/stripping process<sup>[14]</sup>. These factors [Figure 1B] contribute to capacity loss and pose significant safety concerns<sup>[15]</sup>, collectively stifling large-scale commercialization of Li-S batteries.

Efforts have been made to address these challenges, such as designing anchoring hosts<sup>[16]</sup> or modifying separators<sup>[17]</sup>. Early attempts have focused on integrating sulfur into porous carbon-based materials such as graphene foam<sup>[18]</sup>, porous carbon<sup>[19]</sup>, and carbon nanotube (CNT) networks<sup>[20]</sup>, which provide physical confinement for LiPSs. However, the weak intermolecular interactions between nonpolar, hydrophobic carbon hosts and polar, hydrophobic LiPSs are insufficient to prevent the shuttle effect. Alternatively, polar materials such as transition metal oxides, sulfides, and carbides have been proposed to enhance the adsorption of LiPSs, although improvements have been modest<sup>[21-23]</sup>. Recently, strategies targeting the acceleration of the conversion between LiPSs and Li<sub>2</sub>S<sub>2</sub>/Li<sub>2</sub>S have been developed<sup>[24]</sup> by using transition metal compound nanomaterials, including oxides<sup>[25,26]</sup>, sulfides<sup>[27-31]</sup>, selenides<sup>[32,33]</sup>, nitrides<sup>[34-36]</sup>, carbides<sup>[37,38]</sup>, phosphides<sup>[39-41]</sup>, and alloys<sup>[42,43]</sup>. Other effective approaches include modifying separators to confine LiPSs to the cathode side to mitigate the shuttle effect and protect the Li metal anode. Overall, the key strategy aims at integrating functional materials that provide enhanced conductivity, efficient physical or chemical capture of LiPSs, and/or effective catalytic conversion of LiPSs to improve their properties<sup>[44-46]</sup>.

Among the different types of metallic compounds, Molybdenum (Mo), a silver-gray metal obtained as a by-product of copper/tungsten mining, sees China - a global leader in Mo resources - produce over 100,000

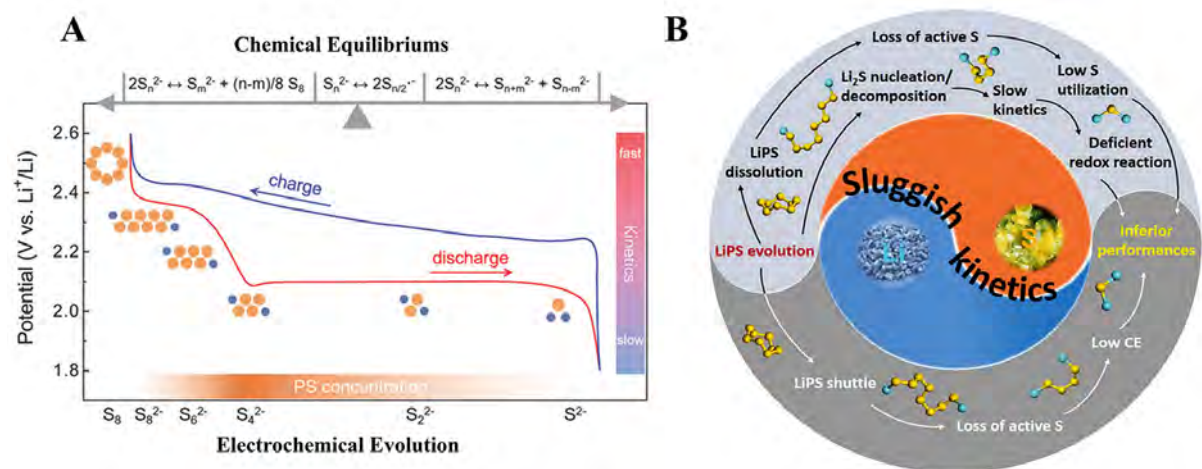


**Figure 1.** Overview of lithium-sulfur batteries and related challenges. (A) Working mechanism of LSBs. Reproduced with permission from Ref. <sup>[11]</sup> Copyright 2018, Wiley-VCH. (B) Main challenges in LSBs. Reproduced with permission from Ref. <sup>[15]</sup> Copyright 2021, Elsevier.

metric tons annually<sup>[47]</sup>. Its Pt-like electronic structure drives unique physicochemical properties, enabling key applications in electrocatalytic hydrogen production and Li-S batteries. Additionally, Mo-based materials have attracted particular attention due to their tunable compositions, adjustable lattice structures, and variable valence states of Mo centers. These characteristics allow for multiple interactions, including polar adsorption, Lewis acid-base interactions, and conversion reactions, to mitigate the shuttle effect associated with LiPSs<sup>[48,49]</sup>. Currently, most related research and reviews concentrate on semiconducting Mo-based materials with conventional electronic structures<sup>[50]</sup>. Nonetheless, The metallic-like electronic structures of MoC<sub>x</sub> and MoN<sub>x</sub> deliver high conductivity (e.g., MoC<sub>x</sub>: ~2,000 S/cm), effectively lowering charge transfer resistance in sulfur cathodes<sup>[51]</sup>. Nonmetallic elements in their Mo-Mo lattices elongate metal bonds and contract Mo d-orbital electrons, raising d-orbital electron density near the Fermi level and imparting Pt-like catalytic activity<sup>[52]</sup>. These properties enable MoC<sub>x</sub> and MoN<sub>x</sub> to act as both conductive scaffolds and catalytic centers, directly mitigating Li-S battery limitations such as polysulfide shuttling, sluggish kinetics, and high-sulfur-loading instability. Although Mo-based nitrides and carbides possess unique physicochemical properties that make them promising candidates for catalysis and energy storage, they have not been extensively reviewed in the context of Li-S batteries.

In this review, we present the first comprehensive overview of the latest advancements in Mo-based nitrides and carbides for Li-S batteries, with a particular focus on their synergistic effects in electrocatalysis, state-of-the-art doping/interface engineering strategies, and future prospects in solid-state devices, we focus on the latest advancements in Mo-based nitrides and carbides for Li-S batteries. We begin by elucidating the physicochemical properties and catalytic activities of these materials, providing detailed discussions of their properties and activities, and highlighting their mechanisms and properties. Subsequently, we examine the design and application of Mo-based nitrides/carbides in Li-S batteries, including their roles as sulfur cathodes and interlayers for separator membranes. We delve into the interactions between these compounds and LiPSs and investigate the fundamental mechanisms for enhanced adsorption and reaction kinetics. Furthermore, we explore how microenvironments in the composite affect the catalytic ability in the conversion of polysulfides. Finally, we discuss the future development and prospects of advanced Mo-based nitrides and carbides for Li-S batteries. By providing a comprehensive overview of Mo-based nitrides and carbides for Li-S batteries, we aim to consolidate existing knowledge, identify research gaps that must be overcome prior to commercialization, and inspire future innovations in energy storage technologies.

## OVERVIEW OF MO-BASED CARBIDES/NITRIDES

Molybdenum carbide  $\text{MoC}_x$  are notable examples of platinum-like, Mo-based compounds, celebrated for their exceptional catalytic activity, which stems from their platinum-like electronic structures.  $\text{MoC}_x$ , as carbides of early transition metals (group IV to VI), are interstitial alloys where carbon atoms are embedded in the lattice interstices of Mo atoms<sup>[53]</sup>. Their crystal phases [Figure 2A] include  $\alpha\text{-MoC}_{1-x}$  ( $0 < x < 0.5$ ),  $\beta\text{-Mo}_2\text{C}$ ,  $\gamma\text{-MoC}$ , and  $\eta\text{-MoC}$ <sup>[54]</sup>. In  $\text{Mo}_2\text{C}$ , carbon atoms fill the interstitial spaces among closely packed Mo atoms on account of their smaller atomic radius compared to metallic Mo. These structural arrangements produce electronic properties dictating both the direction and magnitude of electron transfer between Mo and C atoms and modification to the d-band of metallic Mo atoms<sup>[55]</sup> due to carbon insertion.

Experimental data and theoretical calculations suggest that the Mo-C bond in  $\text{MoC}_x$  exhibits a significant ionic characteristic, with electrons transferring from Mo to C within a range of zero to two electrons. This electron transfer leads to lattice expansion, d-band contraction, and a larger density of states (DOS) near the Fermi level. These band structure changes enhance the surface and adsorption properties, electron transfer, and reaction kinetics. Such characteristics are crucial to the conversion of LiPSs in batteries by mitigating the shuttle effect, a common challenge to Li-S batteries impacting capacity and efficiency. In the meantime, after carbon insertion, the shortest Mo-Mo bond distance expands from 272 to 300 pm, resulting in d-band contraction in metallic Mo and boosting the DOS of Mo atoms near the Fermi level. Comparison of band structure calculations for Mo (110) and Mo-terminated  $\beta\text{-Mo}_2\text{C}$  (100) demonstrates that Mo-C bonding broadens the d-band and redistributes the DOS below ( $< -4$  eV) and above ( $> 3.5$  eV) the Fermi level<sup>[56]</sup>. This redistribution, with the d-band center moving closer to the Fermi level, imparts  $\text{MoC}_x$  with an electronic structure similar to noble metals<sup>[57]</sup> [Figure 2B]. Consequently, the unique electronic structure and catalytic activity of molybdenum carbide make it highly effective in addressing key issues of Li-S batteries, such as improving reaction kinetics and minimizing the shuttle effect, in order to enhance the battery capacity and cycling life for S cathodes.

Similarly,  $\text{MoN}_x$ , structurally related to molybdenum carbides, represents a class of interstitial compounds with solid-state chemical properties akin to the parent metal. Formed by small-radius nitrogen (N) atoms in the Mo atomic lattice,  $\text{MoN}_x$ , as depicted in [Figure 2C], involves Mo atoms adopting face-centered cubic (fcc) and hexagonal close-packed (hcp) structures<sup>[58]</sup>, with N atoms occupying octahedral interstitial sites within both fcc and hcp lattices. The insertion of N atoms introduces tensile strain to the Mo atomic lattice, thus reducing the overlap of adjacent metal atoms' d-bands and increasing the DOS near the Fermi energy level<sup>[59]</sup>. This alteration produces an electronic structure that resembles platinum (Pt) [Figure 2D]. The primary types of bonding in Mo nitride include metallic bonds between Mo atoms, covalent bonds between Mo and N atoms, and ionic bonds formed through charge transfer between Mo and N atoms. Owing to these unique structural properties,  $\text{MoN}_x$  exhibits metallic conductivity, excellent chemical stability, and high catalytic activity, making it widely applicable to Li-S batteries.

## MOLYBDENUM CARBIDE CATALYSTS IN LI-S BATTERIES

### $\text{Mo}_2\text{C}$ catalysts

As discussed above,  $\text{Mo}_2\text{C}$  exhibits excellent metallic conductivity and remarkable catalytic activity due to its platinum-like electronic structure. Recently, it has gained attention as a promising polar catalyst for both catalytic hosts in the cathode and the modified layers on the separators in Li-S batteries. As for the former, Sun *et al.* have synthesized  $\text{Mo}_2\text{C}@C$  as a cathode sulfur host in Li-S batteries<sup>[60]</sup>.  $\text{Mo}_2\text{C}$  undergoes sulfidation upon contact with sulfur to produce a sulfided surface ( $\text{S-Mo}_2\text{C}$ ) with moderate adsorption energy (2-3 eV) and suppressed shuttle effect. Additionally, density-functional theory (DFT) calculations show that the oxidation energy barrier of  $\text{Li}_2\text{S}$  on the sulfided  $\text{Mo}_2\text{C}$  surface is only 0.38 eV, which is

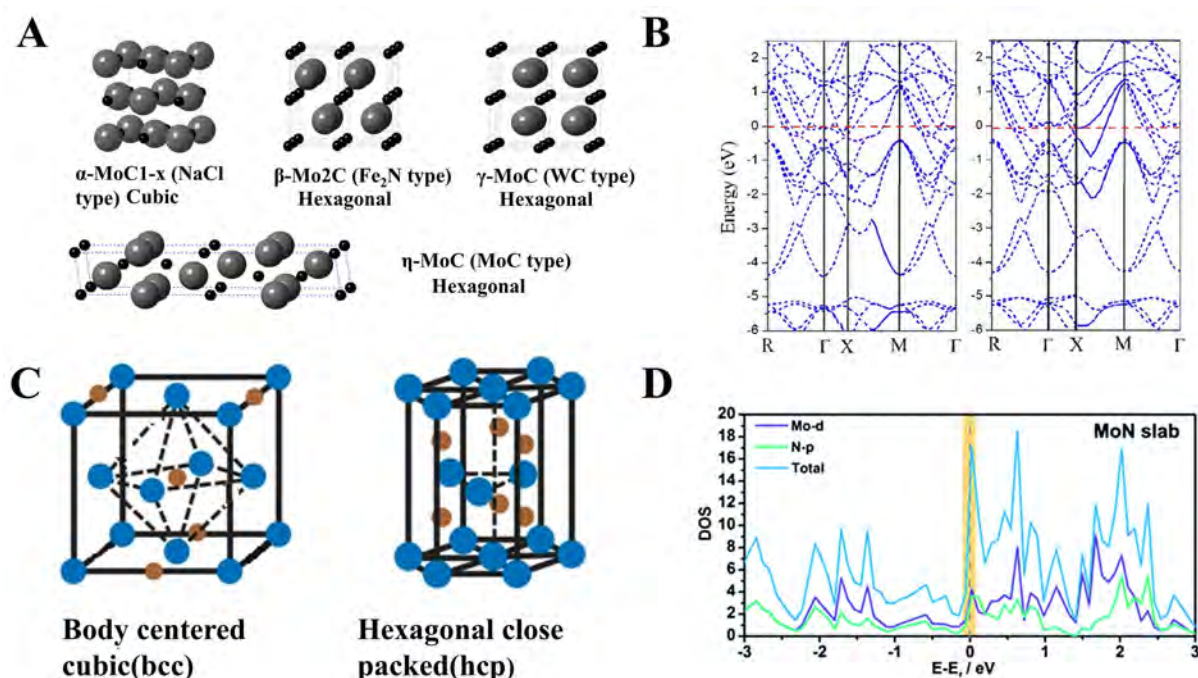


**Figure 2.** Crystal structures and electronic structures of two typical molybdenum carbide and nitride. (A) Crystal structure of molybdenum carbide. Reproduced with permission from Ref.<sup>[54]</sup> Copyright 2014, Wiley-VCH. (B) Electronic band structure of Mo<sub>2</sub>C calculated with (left) VASP and (right) WIEN2k. Reproduced with permission from Ref.<sup>[57]</sup> Copyright 2022, American Chemical Society. (C) Crystal structures of molybdenum nitride. Reproduced with permission from Ref.<sup>[58]</sup> Copyright 2016, Wiley-VCH. (D) Calculated density of states (DOS) of MoN. The orange-shaded areas highlight the DOS contribution near the Fermi level. Reproduced with permission from Ref.<sup>[59]</sup> Copyright 2014, The Royal Society of Chemistry.

significantly lower than that of traditional carbon-based materials. The reduction in the energy barrier accelerates the redox reactions of LiPSs. At a rate of 0.2 C, the initial specific capacity reaches 1,108 mAh g<sup>-1</sup> and retains 76.7% after 200 cycles, demonstrating that Mo<sub>2</sub>C enhances LiPS utilization and improves the properties of Li-S batteries.

However, despite its high catalytic activity, the relatively small specific surface area of Mo<sub>2</sub>C limits the exposure of active sites, resulting in reduced adsorption and catalytic efficiency. Therefore, controlling the particle size of molybdenum carbide while improving its conductivity and dispersibility is theoretically advantageous by exposing more active sites to maximize the electrocatalytic activity in Li-S batteries. For instance, Razaq *et al.* have prepared a composite with Mo<sub>2</sub>C nanoparticles anchored on CNTs (CNT/Mo<sub>2</sub>C) as a sulfur host by annealing CNTs and ammonium molybdate at 800 °C [Figure 3A]<sup>[61]</sup>. Mo<sub>2</sub>C nanoparticles are anchored on CNTs, provide polar sites for LiPSs adsorption and facilitate their conversion [Figure 3B]. The CNT/Mo<sub>2</sub>C/S electrode exhibits a specific capacity of 417 mAh g<sup>-1</sup> at a rate of 2 C after 900 cycles and 52.0% capacity retention. Similarly, Qian *et al.* have introduced highly dispersed Mo<sub>2</sub>C as a conductive polar medium to enhance the electrochemical performance of Li-S batteries based on the hierarchical Mo<sub>2</sub>C nanocluster/carbon nanosheet hybrid hollow sphere [Figure 3C]<sup>[62]</sup>. In this hollow structure, ultrafine Mo<sub>2</sub>C nanocrystals (approximately 2 nm) are confined within carbon nanosheets to aid LiPSs anchoring and mitigate the shuttle effect. Additionally, these electrocatalytic Mo<sub>2</sub>C nanoparticles promote the conversion of LiPSs to Li<sub>2</sub>S<sub>2</sub>/Li<sub>2</sub>S [Figure 3D]. The synergistic effects in Mo<sub>2</sub>C/CHS enhance the electrochemical kinetics in Li-S batteries, even at a high sulfur loading (5 mg cm<sup>-2</sup>) under lean electrolyte conditions (E/S = 7  $\mu$ L mg<sup>-1</sup>).

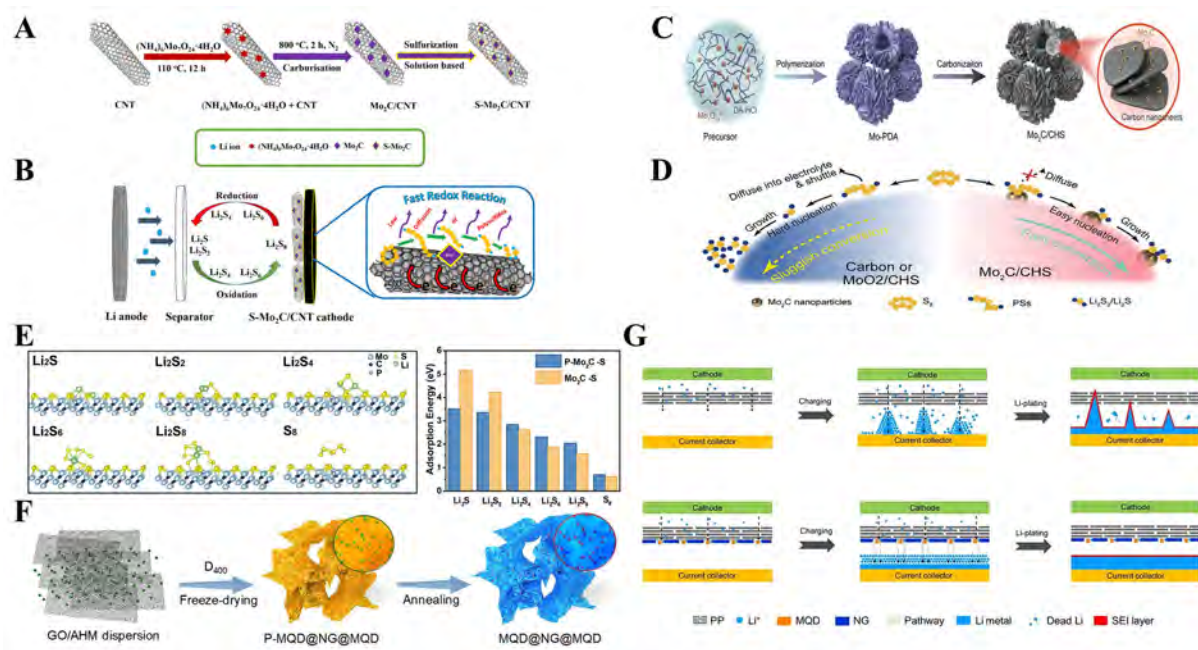


**Figure 3.** Enhancing the properties of LSBs by the host design and separator modification. (A) Schematic illustration of the synthesis process of Mo<sub>2</sub>C/CNT and S-Mo<sub>2</sub>C/CNT. (B) Illustration of the promoted adsorption and the redox reaction of polysulfides on Mo<sub>2</sub>C/CNT for the fast conversion of polysulfides. Reproduced with permission from Ref. [61] Copyright 2018, IOP. (C) Synthesis process of the Mo<sub>2</sub>C/CHS composite. (D) Role of Mo<sub>2</sub>C/HSC in promoting the nucleation and diffusion processes of PSs. Reproduced with permission from Ref. [62] Copyright 2021, Elsevier. (E) Optimized adsorption structures of S<sub>8</sub> and Li<sub>2</sub>Sn on P-Mo<sub>2</sub>C-S substrate and adsorption energy of S<sub>8</sub> and Li<sub>2</sub>Sn on P-Mo<sub>2</sub>C-S and Mo<sub>2</sub>C-S. Reproduced with permission from Ref. [63] Copyright 2024, Elsevier. (F) Dendritic lithium growth in cells with PP separator and MQD@NG@PP separator. (G) Schematic illustration of the synthesis process of MQD@NG. Reproduced with permission from Ref. [68] Copyright 2020, Elsevier.

Further enhancements in the electrochemical activity of Mo<sub>2</sub>C nanomaterials in Li-S batteries have been achieved by ion doping, which induces atomic redistribution and exposes abundant edge sites. For example, Wang *et al.* have synthesized P-doped Mo<sub>2</sub>C nanoparticles anchored on carbon nanofibers (CNFs) by an organic-inorganic nanohybridization process [63]. By modulating the electronic structure of Mo<sub>2</sub>C through phosphorus doping, the electron density increases, and P-Mo<sub>2</sub>C possesses stronger LiPSs adsorption and enhanced sulfur redox kinetics. DFT calculations reveal that there are abundant active sites on the P-doped Mo<sub>2</sub>C surfaces, thereby optimizing both the formation and decomposition processes of Li<sub>2</sub>S. These findings illustrate that P-doped Mo<sub>2</sub>C offers enhanced LiPSs adsorption capabilities and improved sulfur redox kinetics [Figure 3E]. Chen *et al.* engineered B-doped metastable cubic Mo<sub>2</sub>C ( $\delta$ -B-Mo<sub>2</sub>C/NCNT) as a sulfur host [64]. Its 2D nanosheet-assembled tubular structure enables rapid LiPS electron transfer and confinement. DFT calculations reveal B-doping-induced phase transition shifts the Mo d-band center upward, enhancing Mo(d)-S(p) orbital hybridization to accelerate kinetics. The  $\delta$ -B-Mo<sub>2</sub>C/NCNT achieves 606.3 mAh g<sup>-1</sup> at 4.0 C, retains 622.8 mAh g<sup>-1</sup> after 1,000 cycles (1.0 C), and delivers 6.95 mAh cm<sup>-2</sup> under 6.8 mg cm<sup>-2</sup> sulfur loading.

Similarly, Li *et al.* designed cobalt-doped  $\beta$ -Mo<sub>2</sub>C spheres (Co-Mo<sub>2</sub>C@C) as sulfur nano-reactors to optimize the growth of Li<sub>2</sub>S<sub>1/2</sub> and to accelerate the conversion kinetics from Li<sub>2</sub>S<sub>2</sub> to Li<sub>2</sub>S [65]. DFT calculations indicate that Co-Mo<sub>2</sub>C@C exhibits strong interactions with Li<sub>2</sub>S<sub>2</sub>, shortening the Li-S bond length, which makes it more prone to breaking and ultimately forming Li<sub>2</sub>S. Furthermore, Co-Mo<sub>2</sub>C@C lowers the energy barrier for the Li<sub>2</sub>S<sub>2</sub>-to-Li<sub>2</sub>S conversion and enhances both electron transfer and ion diffusion rates. As a result, the Co-Mo<sub>2</sub>C@C/S cathode delivers an excellent specific capacity of 1,200 mAh g<sup>-1</sup> at 0.1 C, and it

also demonstrates outstanding cycling stability.

These examples highlight three doping approaches: anionic (P) and cationic (B). Both strategies modify electronic structures, induce lattice strain, and optimize active sites for synergistic enhancement. Transition metal compounds, leveraging their d-orbital tunability, enable precise band structure adjustments via doping, significantly boosting sulfur redox kinetics.

Building on the effectiveness of Mo<sub>2</sub>C as host materials in enhancing Li-S batteries, attention has been paid to the critical role of the modification of separators<sup>[66,67]</sup>. Positioned between the sulfur cathode and the lithium anode, the separator acts as the sole pathway for the diffusion of soluble LiPSs from the cathode to the anode, earning it the moniker "auxiliary electrode". Recent advancements in separator design enable the suppression of the shuttle effect while improving the electrochemical kinetics of Li-S batteries. Yu *et al.* have performed DFT calculations to predict that Mo<sub>2</sub>C can accelerate Li<sup>+</sup> diffusion to achieve uniform lithium deposition<sup>[68]</sup>. Experimental studies have demonstrated the successful anchoring of P-doped Mo<sub>2</sub>C quantum dots (MQDs) on nitrogen-doped graphene (MQD@NG). These polar MQDs exhibit strong chemical adsorption toward LiPSs and provide rapid diffusion channels for Li<sup>+</sup> transport [Figure 3F and G], consequently facilitating uniform Li<sup>+</sup> flow across the electrode surface and dendrite-free, uniform lithium deposition.

By applying these advancements to Mo<sub>2</sub>C, Li-S batteries deliver enhanced performance, thus addressing key challenges such as the shuttle effect and uniform lithium deposition. This holistic approach underscores the potential of Mo<sub>2</sub>C and innovative separator designs to revolutionize Li-S batteries.

### MoC catalysts

Both hexagonal  $\eta$ -MoC and fcc  $\alpha$ -MoC<sub>1-x</sub> exhibit an ABCABC stacking sequence. Although they have lower electronic conductivity and surface stability compared to the ABAB-stacked  $\beta$ -Mo<sub>2</sub>C with metallic planes, the ABCABC stacking introduces more diverse atomic layer positions, resulting in a greater variety of active sites on the surface. These diverse active sites are effective in adsorbing and activating LiPSs to enhance the catalytic conversion efficiency. Moreover, the complex stacking sequence facilitates the formation of surface defects and edge sites, which typically exhibit higher chemical activity compared with Mo<sub>2</sub>C, contributing to improved adsorption and conversion capabilities for LiPSs. The research associated with the MoC has mainly focused on the design of the nanostructured composite hosts to enhance the exposed catalytic sites. Shi *et al.* have embedded necklace-like MoC nanoparticles into an interconnected CNF network<sup>[69]</sup>. The uniformly distributed MoC nanoparticles serve as chemical traps and electrocatalysts to adsorb LiPSs and accelerate the redox reactions. In addition, the interconnected structure facilitates the rapid transport of Li<sup>+</sup> and electrons throughout the electrode, which is particularly beneficial for cathodes with high sulfur loading [Figure 4A and B]. As a result, the MoC@N-CNF/Li<sub>2</sub>S<sub>6</sub> electrode has a stable high areal capacity of 12.3 mAh cm<sup>-2</sup> at a large sulfur loading of 10 mg cm<sup>-2</sup> at a 0.1 C rate.

Downsizing molybdenum carbide (MoC) to enhance its specific surface area through microstructure and nanostructure design is inherently constrained. While higher MoC loadings allow for the rapid conversion of adsorbed LiPSs, the effectiveness of this process is significantly hampered by the smaller number of active sites and surface area. This limitation ultimately compromises the catalytic efficiency of the MoC. Therefore, it is crucial to determine the optimal MoC loading on the cathode to optimize the catalytic activity. Ji *et al.* have fabricated CNFs@MoC composites with different MoC loadings using electrospinning combined with carbothermal reduction<sup>[70]</sup>. By adjusting the calcination temperature and molybdenum acetylacetonate content, the adsorption of LiPSs is improved with increasing MoC loading. Among the

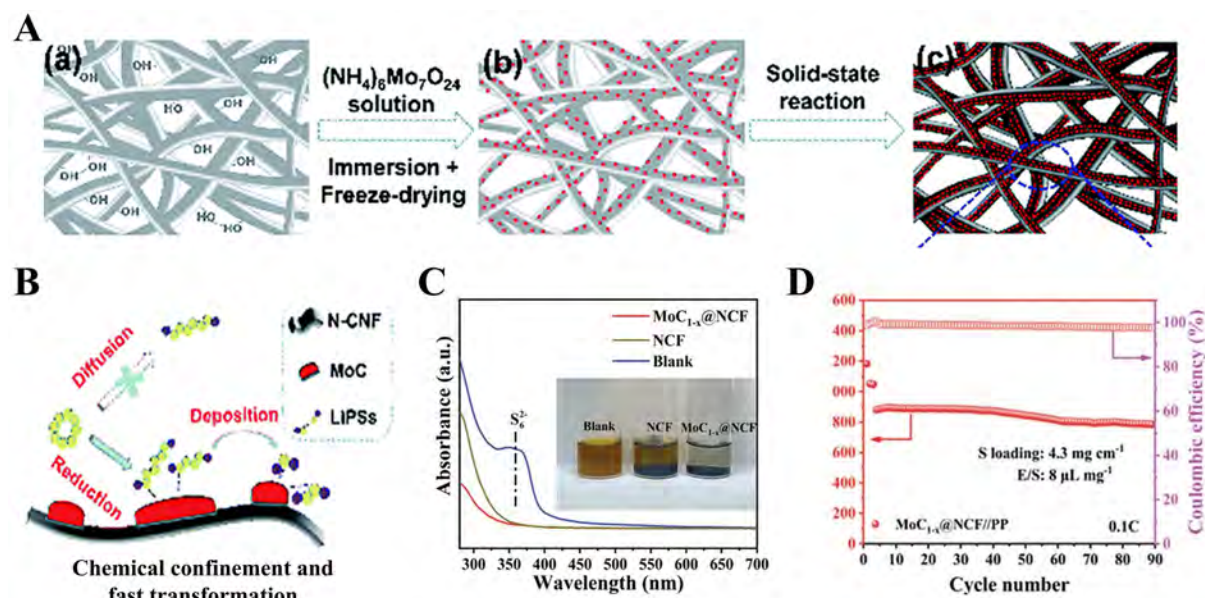


**Figure 4.** MoC<sub>x</sub>-based electrocatalyst used for LSBs. (A) Schematic diagram of the preparation of the MoC@N-CNF freestanding electrode. (B) Role of necklace-like MoC in LiPS immobilization and transformation. Reproduced with permission from Ref.<sup>[69]</sup> Copyright 2019, The Royal Society of Chemistry. (C) Static adsorption experiment of MoC<sub>1-x</sub>@NCF and NCF in Li<sub>2</sub>S<sub>6</sub> solution and corresponding UV-vis absorption spectrum. (D) Cyclic characteristics of MoC<sub>1-x</sub>@NCF//PP cell at 0.1 C with a high sulfur loading and lean electrolyte. Reproduced with permission from Ref.<sup>[71]</sup> Copyright 2023, Wiley-VCH.

various composites, CNFs@MoC-37% has the highest Li<sub>2</sub>S deposition capacity (644 mAh g<sup>-1</sup>) and shortest nucleation time (504 s). Additionally, batteries assembled with CNFs@MoC-37%/Li<sub>2</sub>S cathodes maintain a discharge capacity of 550 mAh g<sup>-1</sup> after 500 cycles at 1 C.

Similar to Mo<sub>2</sub>C, MoC is also used to modify the separator as a barrier to alleviate the shuttle effect. For instance, Li *et al.* have synthesized highly dispersed  $\alpha$ -phase molybdenum carbide nanocrystals embedded in a porous nitrogen-doped carbon framework ( $\alpha$ -MoC<sub>1-x</sub>@NCF) using the MOFs as templates<sup>[71]</sup>. These composites are employed as multifunctional interlayers for separators in Li-S batteries. Benefiting from the synergistic capture and catalytic effects of the MoC<sub>1-x</sub>@NCF interlayer on LiPSs [Figure 4C], even at high sulfur loading (6.0 mg cm<sup>-2</sup>) and lean electrolyte conditions (E/S  $\approx$  5.8  $\mu$ L mg<sup>-1</sup>) [Figure 4D], the assembled Li-S batteries show an exceptionally high capacity of 5.2 mAh cm<sup>-2</sup>.

### Mo<sub>2</sub>C/MoC heterostructure catalysts

Mo<sub>2</sub>C and MoC have distinct advantages and limitations in Li-S batteries, and their integration can yield superior performance. Mo<sub>2</sub>C, characterized by its ABAB stacking pattern, boasts high metallic conductivity, excellent surface stability, rapid electron transport, and efficient polysulfide conversion. However, the limited range of active sites may constrain its effectiveness in adsorbing and catalyzing LiPSs. Conversely, MoC with the ABCABC stacking offers a diverse array of active sites and promotes the formation of surface defects to enhance LiPSs adsorption and catalytic conversion. Despite these benefits, the lower electronic conductivity and surface stability of MoC compared to Mo<sub>2</sub>C can degrade the electrochemical properties. The Mo<sub>2</sub>C/MoC heterostructure capitalizes on the strength of both materials<sup>[72]</sup> to deliver enhanced conductivity, abundant active sites, and better LiPSs management to address the shuttle effect, improve sulfur utilization, and enable stable long-term cycling. The synergistic effects at the interface further boost the catalytic performance and structural stability, rendering Mo<sub>2</sub>C/MoC heterostructures a promising solution for high-performance Li-S batteries.

For instance, Han *et al.* have designed a mixed-valence nanoscale Mo<sub>2</sub>C-MoC/C cathode for Li-S batteries, where the mixed valence (Mo<sup>2+</sup> and Mo<sup>3+</sup>) within the Mo<sub>2</sub>C-MoC structure significantly enhances the electrical conductivity and reaction kinetics to counteract the insulating nature of sulfur and lithium sulfide<sup>[73]</sup>. This structure shows stronger adsorption and catalytic conversion activity for polysulfides than single-valence Mo<sub>2</sub>C, yielding an initial discharge capacity of 870.4 mAh·g<sup>-1</sup> at 0.2 C, compared to 620.8 mAh·g<sup>-1</sup> for Mo<sub>2</sub>C/S. Liu *et al.* have synthesized Mo<sub>2</sub>C-MoC heterostructures by high-temperature pyrolysis of MoZn MOF composites to create tri-active regions that synergistically promote charging and discharging processes<sup>[74]</sup>. The Mo<sub>2</sub>C/MoC-S cathode achieves a remarkable capacity of 1,603.6 mAh g<sup>-1</sup> and 80.4% capacity retention after 1,000 cycles at a 3 C rate, thus significantly outperforming batteries catalyzed solely by Mo<sub>2</sub>C or MoC.

## MOLYBDENUM NITRIDE CATALYSTS IN LI-S BATTERIES

### Mo<sub>2</sub>N catalysts

Spurred by the advancements in Molybdenum carbides for Li-S batteries, molybdenum nitride (Mo<sub>2</sub>N) emerges as another candidate offering exceptional catalytic activity and chemical stability rivaling noble metals. The remarkable properties of Mo<sub>2</sub>N stem from its unique electronic structure shaped by Mo-N bonds in the crystal lattice. During the formation of the Mo-N bond, nitrogen atoms occupy interstitial sites of the molybdenum lattice and expand the interatomic distance between adjacent Mo atoms. The restructuring significantly enhances the DOS near the Fermi level, leading to active electron transfer properties and positioning Mo<sub>2</sub>N as an excellent catalyst material. For instance, Jiang *et al.* have synthesized mesoporous Mo<sub>2</sub>N with an average pore size of 8.6 nm using silica as a template with strong adsorption capabilities for LiPSs [Figure 5A and B]<sup>[75]</sup>. This mesoporous structure has superior electrochemical characteristics such as high-capacity retention of 92.0% (914 mAh·g<sup>-1</sup>) after 100 cycles at 0.5 C, which outperforms non-porous Mo<sub>2</sub>N cathodes.

To further enhance the catalytic properties of Mo<sub>2</sub>N, quantum dots (QDs) have been introduced to take advantage of the abundant active sites and redox catalytic activity. Ma *et al.* have constructed Mo<sub>2</sub>N QDs anchored on N-doped graphene oxide (Mo<sub>2</sub>N@NG) by simple reflux-calcination [Figure 5C and D] to serve as a multifunctional interlayer on the polypropylene (PP) separator<sup>[76]</sup>. The well-dispersed Mo<sub>2</sub>N QDs in the NG framework exhibit strong chemical adsorption and affinity toward Li<sup>+</sup> [Figure 5E], as well as excellent electrocatalytic activity for LiPSs conversion. Cyclic voltammetry reveals that the Mo<sub>2</sub>N@NG electrode outperforms the NG electrode with a larger peak area and higher current response, confirming its ability to accelerate the anchoring-diffusion-transformation process of LiPSs [Figure 5F]. This design suppresses the shuttle effect and enhances the redox kinetics, leading to improved sulfur utilization and stable cycling characteristics.

However, despite these advancements, optimizing the intrinsic catalytic activity of Mo<sub>2</sub>N remains critical for achieving high-energy-density Li-S batteries with reduced electrocatalyst loadings. Engineering atomic vacancies is a powerful strategy to modulate the electronic structure of Mo<sub>2</sub>N and enhance both the chemisorption and catalytic conversion of LiPSs. Yang *et al.* have synthesized nitrogen vacancy-rich Mo<sub>2</sub>N QDs (QMo<sub>2</sub>N-V) by spray drying<sup>[77]</sup>. These QDs are integrated into mesoporous carbon microspheres and act as efficient microreactors to capture diffusing LiPSs and facilitate sulfur reutilization. DFT calculations reveal that nitrogen vacancies shift the d-band center of Mo<sub>2</sub>N from -1.90 to -1.66 eV [Figure 5G] to improve LiPSs adsorption and reaction kinetics [Figure 5H and I]. Li-S batteries with QMo<sub>2</sub>N-V-modified separators show a reversible capacity of 510 mAh·g<sup>-1</sup> for 400 cycles at 4.0 C and an impressive areal capacity of 6.6 mAh·cm<sup>-2</sup> for a high sulfur loading (8.1 mg·cm<sup>-2</sup>) and lean electrolyte conditions [Figure 5J]. Similarly, Cheng *et al.* have synthesized oxygen-modified Mo<sub>2</sub>N nanoclusters (C-Mo<sub>2</sub>N-O) by metal-organic

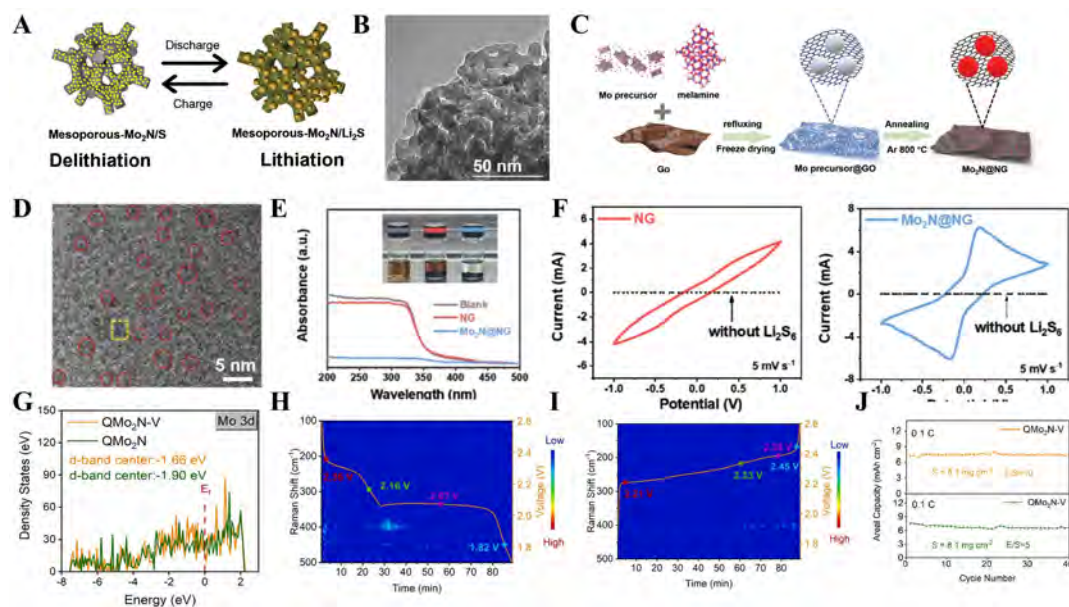


**Figure 5.** Mo<sub>2</sub>N used as an effective sulfur host or interlayer for LSBs. (A) Charging/discharging process of the mesoporous Mo<sub>2</sub>N/S cathode. (B) TEM image of mesoporous Mo<sub>2</sub>N. Reproduced with permission from Ref.<sup>[75]</sup> Copyright 2018, Elsevier. (C) Schematic diagrams of the synthesis of Mo<sub>2</sub>N@NG. (D) High-resolution TEM image of Mo<sub>2</sub>N@NG. (E) Schematic illustration of the preparation stages for MoS<sub>2</sub> QDs-NRGO. (F) Cyclic voltammetry curves of the Li<sub>2</sub>S<sub>6</sub> symmetric cell. Reproduced with permission from Ref.<sup>[76]</sup> Copyright 2022, Wiley-VCH. (G) PDOS of QMo<sub>2</sub>N and QMo<sub>2</sub>N-V. (H-J) *In situ* time-resolved Raman contour mappings of the cells charged and discharged at 0.5 C with QMo<sub>2</sub>N-V modified separators. H Discharging and H charging J Cycling properties of QMo<sub>2</sub>N-V. Reproduced with permission from Ref.<sup>[77]</sup> Copyright 2022, Elsevier.

coordination polymerization to uniformly load the clusters onto the mesoporous carbon sphere frameworks<sup>[78]</sup>. Guided by the Sabatier principle, the surface oxygen atoms weaken the interactions between sulfur species and Mo atoms to balance the adsorption strength and avoid site poisoning. This moderated interaction promotes efficient reversible catalysis. All in all, advancements of Mo<sub>2</sub>N by means of structural engineering (e.g., mesoporous frameworks, QDs, and atomic vacancies) highlight its transformative potential in addressing the challenges of polysulfide management in the pursuit to achieve superior capacity retention and the practical deployment of high-sulfur-loading Li-S batteries.

### MoN catalysts

The molybdenum nitride phase, MoN, has garnered attention for its distinct advantages. While Mo<sub>2</sub>N has remarkable chemical stability, strong LiPSs adsorption, and enhanced catalytic activity, MoN, with its hexagonal close-packed (HCP) structure, brings additional benefits such as its highly ordered atomic arrangement, superior electrical conductivity, and elevated Mo oxidation state. These properties render MoN a promising candidate to further improve the electron transport and catalytic efficiency in Li-S batteries. Liu *et al.* have embedded MoN QDs into a dual-channel ordered mesoporous carbon composite (MoN@CMK-5)<sup>[79]</sup>. The carefully designed bimodal pore structure of MoN@CMK-5 offers a large specific surface area and enhanced electrolyte mass transport, while the high intrinsic catalytic activity facilitates the rapid conversion of polysulfides. This "adsorption-conversion-mass transport" synergy gives rise to outstanding electrochemical characteristics, including an initial capacity of 1,582 mAh·g<sup>-1</sup> at 0.1 C and a capacity decay rate of just 0.027% per cycle after 1,000 cycles at 5 C [Figure 6A]. Furthermore, theoretical calculations reveal that MoN@CMK-5 has a low activation energy for Li<sub>2</sub>S decomposition [Figure 6B and C], consequently suppressing the shuttle effect and stabilizing long-term cycling.

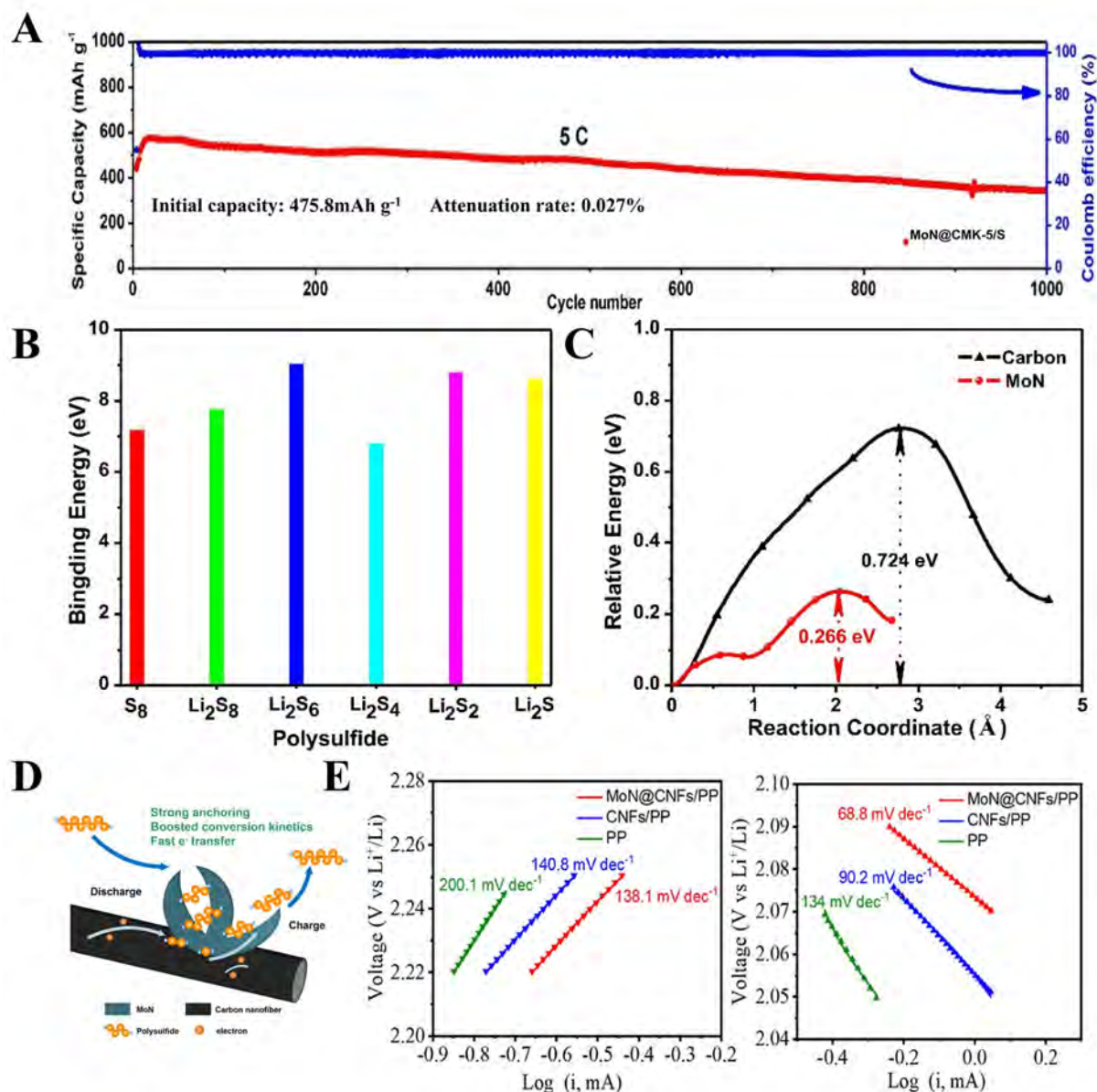


**Figure 6.** MoN used as an effective sulfur host or interlayer for LSBs. (A) Cyclability of MoN-X@CMK-5 at 5 C. (B) Binding energy for different polysulfides for MoN materials. (C) Reaction energy barrier of  $\text{Li}_2\text{S} \rightarrow \text{LiS} + \text{Li}^+$  harvested from carbon and MoN substrates. Reproduced with permission from Ref.<sup>[79]</sup> Copyright 2022, Elsevier. (D) Schematic illustration of the polysulfide anchoring and enhanced conversion on the surface of exposed MoN nanosheets. (E) Oxidation peak I ( $\text{Li}_2\text{S} \rightarrow \text{Li}_2\text{S}_x$ ) and reduction peak IV ( $\text{Li}_2\text{S}_x \rightarrow \text{Li}_2\text{S}$ ). Reproduced with permission from Ref.<sup>[80]</sup> Copyright 2022, American Chemical Society.

In comparison with QDs, 2D materials excel in creating continuous conductive networks, suppressing polysulfides through large and stable interfaces, and providing better structural stability and scalability. They are particularly suitable due to their long-term cycling stability and large-scale electrode fabrication. Tan *et al.* have synthesized molybdenum nitride nanosheets (MoN@CNFs) on CNFs [Figure 6D]<sup>[80]</sup>. The unique nanosheet morphology provides abundant active sites, and the interconnected CNF network ensures efficient electron transport. MoN@CNFs exhibit the smallest Tafel slopes during oxidation and reduction [Figure 6E] and reduce reaction polarization to accomplish bifunctional catalytic activity. As a result, the Li-S battery with MoN@CNFs shows a high initial capacity ( $1,074 \text{ mAh}\cdot\text{g}^{-1}$  at 0.2 C), excellent cycling stability,

and capacity decay as low as 0.055% per cycle at 2 C. These findings highlight the versatility of the MoN as an electrocatalyst, which is capable of accelerating both polysulfide reduction and  $\text{Li}_2\text{S}$  oxidation for better sulfur redox conversion efficiency.

To further optimize bifunctional catalysis for high-performance Li-S batteries, Li *et al.* have fabricated a layered MoN-C-MoN structure to leverage the strong adsorption capability and high catalytic activity while enhancing electron transport through the conductive carbon sheets<sup>[81]</sup>. This layered design maximizes surface exposure for adsorption and catalysis and promotes efficient bidirectional conversion between S and  $\text{Li}_2\text{S}$  with minimal reaction overpotentials [Figure 7A and B].

Liu *et al.* prepared  $\text{MoX}_n$  ( $X = \text{O}, \text{S}, \text{N}, \text{and P}$ ) compounds featuring fixed Mo cations and various anions, and investigated the influence of these anions' p-bands on Li-S electrochemistry<sup>[82]</sup>. DFT calculations reveal that shifting the p-band center leads to different interfacial electron-transfer dynamics, resulting in diverse catalytic activities for polysulfide conversion. The results show that Li-S batteries with a MoN-modified separator exhibit relatively better electrochemical performance, attributed to the narrower energy gap between the metal 3d center and the anion 2p center in MoN compared to the other compounds. Both experimental and computational data confirm that this narrow band gap effectively lowers the decomposition barrier of  $\text{Li}_2\text{S}$ . In particular, the significantly improved kinetics further enhances overall performance [Figure 7C and D].

In addition to the intrinsic advantages, the catalytic activity of MoN can be further improved by metal heteroatom doping, which modulates its electronic structure and enhances LiPSs adsorption and conversion. Kong *et al.* have synthesized Co/ $\text{Mo}_2\text{N}$  composites using a hydrothermal and ammonia nitridation approach<sup>[83]</sup>. The combination of Co and MoN provides synergistic effects to improve the  $\text{Li}_2\text{S}$  nucleation kinetics and sulfur redox reactions. [Figure 8A confirms  $\text{Co} \rightarrow \text{MoN}$  electron transfer (yellow/blue regions: accumulation/depletion), creating a built-in field that streamlines electron transport for LiPSs redox. MoN shows superior  $\text{Li}_2\text{S}$  adsorption (-3.28 eV), preventing intermediate loss. [Figure 8B reveals MoN lowers  $\text{Li}_2\text{S}_2 \rightarrow \text{Li}_2\text{S}$  conversion energy barriers ( $\Delta G$ ), a rate-limiting step. Reduced barriers accelerate kinetics, enhancing battery performance (capacity, rate capability). As a result, the Li//Li symmetrical cell with Co/ $\text{Mo}_2\text{N}$ -coated separators shows stable plating and stripping for 800 h.

In summary, MoN builds upon the successes and limitations of  $\text{Mo}_2\text{N}$  by offering superior conductivity and catalytic activity, making it a powerful candidate for next-generation Li-S batteries. Through innovative structural designs, such as mesoporous composites and carbon-based hybrids, along with electronic modulation strategies such as heteroatom doping, MoN has significant potential to address the challenges posed by polysulfide management, sulfur utilization, and long-term cycling stability.

### Mo<sub>2</sub>N/MoN heterostructures catalysts

$\text{Mo}_2\text{N}$  and MoN are both promising materials for Li-S batteries due to their excellent catalytic properties and high electrical conductivity, which enhance the conversion kinetics of LiPSs and improve overall battery performance.  $\text{Mo}_2\text{N}$  is particularly noted for its strong polysulfide adsorption capabilities<sup>[84]</sup> which help mitigate the shuttle effect, while MoN provides robust structural stability and mechanical strength<sup>[85]</sup>. However, individually, these materials face challenges such as limited surface area and potential stability issues under prolonged cycling conditions. In the process of preparing  $\text{MoN}_x$  through nitridation, insufficient nitridation often results in a mixed phase of  $\text{Mo}_2\text{N}$  and MoN, leading to the formation of abundant grain boundaries between them. These grain boundaries play a crucial role in modulating the surface electronic structure and enhancing catalytic adsorption capabilities<sup>[86,87]</sup>. By building  $\text{Mo}_2\text{N}/\text{MoN}$

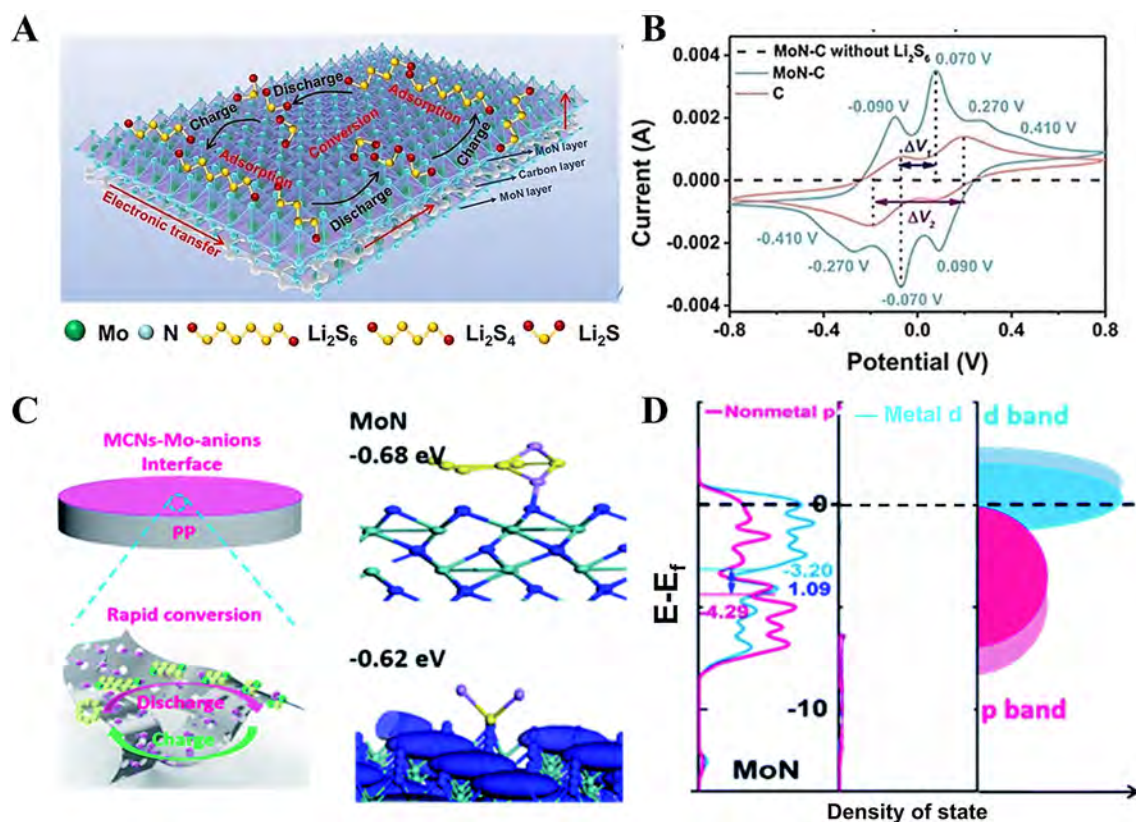


**Figure 7.** Application of molybdenum nitride with bidirectional catalytic functionality in LSBs. (A) Schematic illustration of bifunctional catalysis for MoN-C-MoN. (B) CV curves of symmetrical cells. Reproduced with permission from Ref.<sup>[81]</sup> Copyright 2020, Wiley-VCH. (C) Schematic Illustration of bifunctional catalysis for MCN-Mo and binding energy and electron cloud density after MoN Adsorption. (D) Fermi Level of MoN. Reproduced with permission from Ref.<sup>[82]</sup> Copyright 2022, The Royal Society of Chemistry.

heterostructures, we can leverage the complementary strengths of both materials - combining their catalytic efficiencies, electrical conductivity, and adsorption properties - while addressing their individual limitations. This synergistic approach can result in enhanced reaction kinetics, improved structural integrity, and, ultimately, more efficient and durable Li-S batteries.

For instance, Yang *et al.* synthesized hollow microspheres composed of an MoN-Mo<sub>2</sub>N heterostructure rich in grain boundaries<sup>[88]</sup>. These grain boundaries serve as 2D nucleation sites, exhibiting strong and rapid adsorption abilities toward LiPSs and guiding the deposition of Li<sub>2</sub>S around them, thereby effectively preventing catalyst surface passivation. Consequently, these hollow microspheres enable high-capacity Li<sub>2</sub>S deposition and significantly enhance the conversion kinetics of LiPSs. In assembled batteries featuring an interlayer of these microspheres and CNTs, they demonstrated a low capacity decay of 0.049% per cycle at 1 C for 800 cycles and achieved a high capacity of 698 mAh g<sup>-1</sup> at 4 C.

### MOC<sub>x</sub>/MON<sub>x</sub>-CONDUCTIVE COMPOUND COMPOSITE CATALYSTS

Although nanosized MoC<sub>x</sub> and MoN<sub>x</sub> exhibit remarkable catalytic abilities for converting polysulfides, they tend to aggregate into larger particles with decreased electrochemical activity. Hence, MoC<sub>x</sub> and MoN<sub>x</sub> are typically integrated into a conductive framework, such as carbon materials and metallic compounds, to enhance stability. The catalytic activity of MoC<sub>x</sub> and MoN<sub>x</sub> composites is influenced by the chemical and coordination environments. The chemical environment, which includes different phases or dopants, can

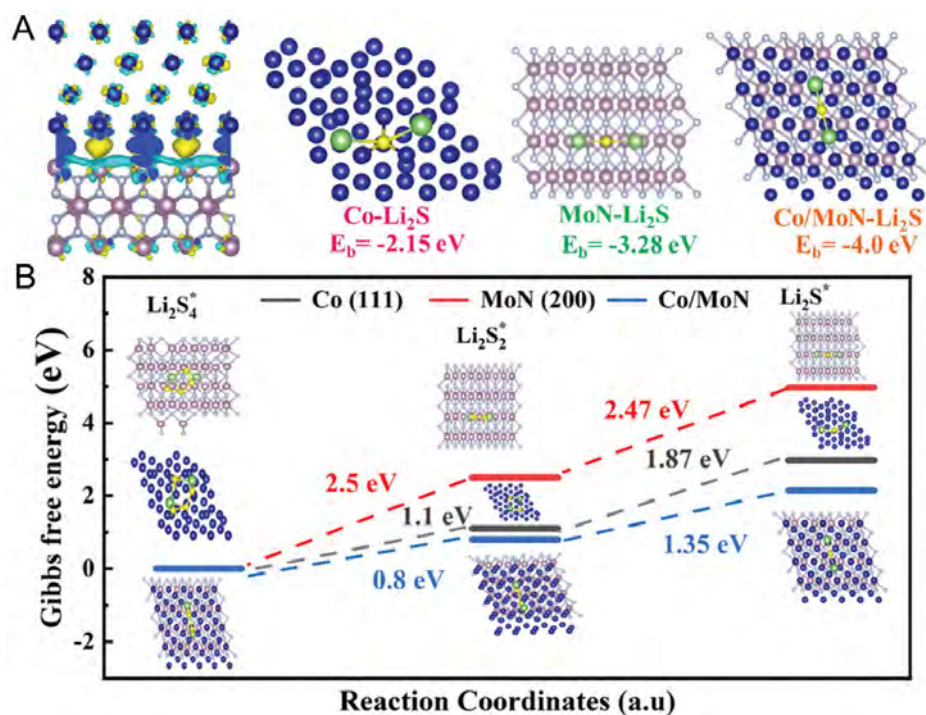


**Figure 8.** DFT of Co/Mo<sub>2</sub>N (A) Charge density difference between Co and MoN (yellow/blue regions indicate electron accumulation/depletion) and optimized Li<sub>2</sub>S configurations and binding energies on Co, MoN, and Co/MoN. (B) Gibbs free energy of LiPSs conversion on Co (111), MoN (200), and Co/MoN; insets: LiPSs adsorption geometries on each surface. Reproduced with permission from Ref.<sup>[83]</sup> Copyright 2023, Wiley-VCH.

modify the electronic properties to improve the interactions between the catalyst and reactants. The coordination environment, defined by the arrangement of atoms around active sites, impacts their accessibility and reactivity and promotes more efficient catalytic reactions. Furthermore, synergistic interactions in MoC<sub>x</sub> and MoN<sub>x</sub> composites can lead to the development of new active sites, combining the electrical conductivity of MoC<sub>x</sub> with the adsorption capabilities of MoN<sub>x</sub>. By thoroughly investigating the microenvironments in the composite, it is possible to improve the catalytic ability and efficiency in applications such as energy storage and conversion systems.

### MoC<sub>x</sub>/MoN<sub>x</sub>-carbon composites

Combining carbon materials with MoC<sub>x</sub> and MoN<sub>x</sub> to fabricate MoC<sub>x</sub>/MoN<sub>x</sub>-carbon composites offers significant benefits, particularly for Li-S batteries. Carbon materials possess a high intrinsic surface area, which provides more active sites for catalytic reactions and facilitates the interactions between the catalyst and reactants to improve the efficiency of energy conversion and storage. However, designing micro and nanostructures to increase the surface area of MoC<sub>x</sub>/MoN<sub>x</sub> is still challenging. As the sulfur concentration or areal loading in the cathode increases, the availability of sulfur hosting sites becomes insufficient and furthermore, the persistent LiPSs shuttling effect during long-term cycling severely compromises the battery lifetime.

Owing to the large specific surface area and excellent electrical conductivity of carbon materials, integrating MoC<sub>x</sub>/MoN<sub>x</sub> with carbon presents an effective strategy to improve the properties of Li-S batteries. Three-dimensional (3D) carbon architectures with optimized pore structures are the ideal substrates as they allow large sulfur loading and accommodate the volumetric expansion during cycling. For instance, Niu *et al.* have designed a freestanding Mo<sub>2</sub>C/graphene/N-doped carbon foam composite (GCF-G@Mo<sub>2</sub>C) featuring

an agar-like porous structure<sup>[89]</sup>. Here, graphene sheets wrapped around N-doped carbon bubbles enable rapid electron and ion transport. Experiments and first-principles calculations reveal that the Mo<sub>2</sub>C nanoparticles, acting as chemical anchoring centers, exhibit a high affinity for polysulfides and accelerate the redox conversion through catalytic effects. Consequently, the GCF-G@Mo<sub>2</sub>C battery shows an initial capacity of 862 mAh g<sup>-1</sup> and maintains a capacity of 597 mAh g<sup>-1</sup> after 600 cycles at 1 C, with a decay rate of only 0.051%, demonstrating excellent cycling stability.

The porous structure of carbon enhances its catalytic ability by increasing the surface area, improving mass transport, and ensuring efficient dispersion and accessibility of active sites. MOFs, with their well-defined porous structures and crystallinity, offer an alternative approach to constructing 3D porous carbon architectures. Wang *et al.* have synthesized MoN@N-doped carbon (MoNNC) porous octahedra using a MOF precursor by high-temperature thermal annealing, etching, and nitridation [Figure 9A]<sup>[90]</sup>. Cyclic voltammetry conducted on the symmetrical cell in the Li<sub>2</sub>S<sub>6</sub>-containing electrolyte demonstrates that MoNNC promotes the chemisorption and conversion of LiPSs. The MoNNC/S cathode, with a 77.0 wt% sulfur loading, shows a capacity retention of 88.0% at 0.5 C and maintains a reversible capacity of 934 mAh·g<sup>-1</sup> after 100 cycles, which outperform MoN/S and NC/S. Chen *et al.* have developed porous nano-octahedron (Mo<sub>2</sub>C-C NOs) with ultrafine Mo<sub>2</sub>C nanocrystals embedded in a porous carbon substrate as sulfur hosts for Li-S batteries<sup>[91]</sup>. The large surface area and pore volume of Mo<sub>2</sub>C-C NOs accommodate sulfur infiltration and buffer volume changes. Additionally, the polar Mo<sub>2</sub>C chemically adsorbs LiPSs through strong Mo-S bonds, and the electrocatalytic activity enhances the redox kinetics of sulfur species.

In practical applications of Li-S batteries, the economic significance of large-scale, controllable synthesis of heteroatom-doped carbon materials must be considered. Using a biological carbon source, Wang *et al.* have prepared ultrafine Mo<sub>2</sub>C nanocrystals anchored on a bio-oil-derived 3D layered carbon matrix (Mo<sub>2</sub>C@BOC) by NaCl template-assisted electrostatic self-assembly and subsequent annealing [Figure 9B]<sup>[92]</sup>. This method facilitates the mixing of Mo<sup>5+</sup> and bio-oil feedstocks on a molecular scale to reduce the crystal size of Mo<sub>2</sub>C in the final product. This reduction in size increases the exposure of active sites to enhance the catalytic activity. Constant-potential discharge tests reveal that the Mo<sub>2</sub>C@BOC electrode achieves the highest deposition capacity and the shortest nucleation time [Figure 9C], confirming that the high conductivity and effective catalytic activity significantly enhance the kinetics of LiPSs conversion to Li<sub>2</sub>S.

### MoC<sub>x</sub>/MoN<sub>x</sub>-metallic compound composites

In addition to carbon materials, integrating metallic compounds with MoC<sub>x</sub> and MoN<sub>x</sub> in Li-S battery composites can address several key challenges in battery technology. The integration enhances the catalytic activity, electrical conductivity, and structural stability, leading to more efficient and durable energy storage. Typically, single materials have limited adsorption and catalytic capabilities for LiPSs. However, by constructing heterostructures composed of two different metal compounds, the chemical confinement and conversion of polysulfides are synergistically enhanced<sup>[93,94]</sup>. These materials with heterostructures possessing superior electrical properties can be directly used as electrode materials or additives to boost the battery performance. For instance, in Li-S batteries, heterostructures help anchor LiPSs and catalyze the accelerated conversion through the built-in electric fields to achieve the synergistic "adsorption-catalysis" effect. Unlike alloying, which combines multiple metals, heterostructure engineering involves hybridizing different types of compounds with tightly bonded interfaces<sup>[95]</sup>.

As discussed previously, MoC<sub>x</sub>/MoN<sub>x</sub> exhibits high conductivity and catalyzes the rapid conversion of LiPSs in Li-S batteries. In heterostructures based on highly conductive transition metal compounds, electrons

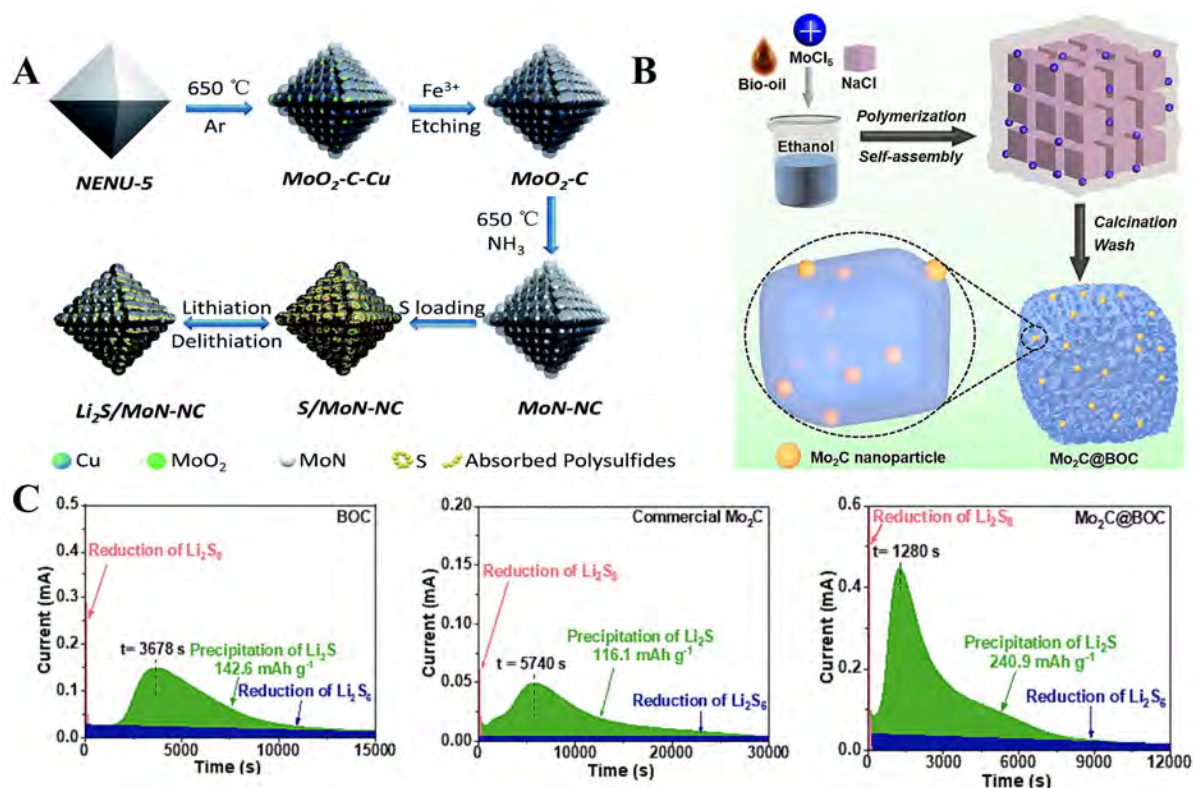


**Figure 9.** Application of Mo<sub>x</sub>/Mo<sub>n</sub> composites with high-specific-surface-area carbon materials in Li-S batteries. (A) Synthesis process for MoN-NC. Reproduced with permission from Ref.<sup>[90]</sup> Copyright 2019, The Royal Society of Chemistry. (B) Schematic illustration of fabrication strategy of Mo<sub>2</sub>C@BOC host. (C) Precipitation profiles of Li<sub>2</sub>S. Reproduced with permission from Ref.<sup>[92]</sup> Copyright 2023, Elsevier.

transfer swiftly along the heterointerface. The distinct components of the heterojunction create an intrinsic electric field that facilitates rapid Li<sup>+</sup> diffusion, resulting in superior catalytic performance. For instance, Zhao *et al.* have developed Mo<sub>2</sub>N-MoC/NC nanomaterials with dense heterointerfaces<sup>[96]</sup>. The Mo<sub>2</sub>N-MoC interface generates a strong built-in electric field to enhance electron migration and the redox reactions of LiPSs [Figure 10A and B]. These properties make Mo<sub>2</sub>N-MoC/NC nanobelts ideal for separator modification, effectively capturing, diffusing, and converting soluble LiPSs into solid Li<sub>2</sub>S<sub>2</sub>/Li<sub>2</sub>S. Consequently, batteries with the modified separator achieve an initial discharge capacity of 1,507.8 mAh g<sup>-1</sup> and excellent long-term cycling stability by retaining 623.6 mAh g<sup>-1</sup> after 700 cycles with a capacity fade rate of only 0.058% per cycle [Figure 10C]. Similarly, Zhang *et al.* have synthesized two-dimensional Mo<sub>2</sub>C-Mo<sub>2</sub>N/C composites using an *in situ* nitridation strategy assisted by g-C<sub>3</sub>N<sub>4</sub>, as modification layers in commercial Li-S battery separators<sup>[97]</sup>. Experimental studies and DFT calculations reveal that the heterostructured Mo<sub>2</sub>C-Mo<sub>2</sub>N materials enhance the adsorption of dissolved LiPSs through Mo-S and Li-N bonds while accelerating the reduction with the built-in electric field. As a result, the Li-S battery with Mo<sub>2</sub>C-Mo<sub>2</sub>N/C/PP separators shows a discharge capacity of 1,404 mAh g<sup>-1</sup> at 0.1 C and maintains 623.6 mAh g<sup>-1</sup> after 700 cycles at 1 C, with a capacity fade rate of only 0.028% per cycle.

Metallic compounds forming Mott-Schottky heterojunctions with specific compounds enable spontaneous charge migration and separation at the interface, leading to electron enrichment on one side and generation of abundant holes on the other side to create an intrinsic electric field that enhances the redox conversion of LiPSs by optimizing the interfacial electronic structure<sup>[98,99]</sup>. For example, Li *et al.* have synthesized Mo<sub>2</sub>C-

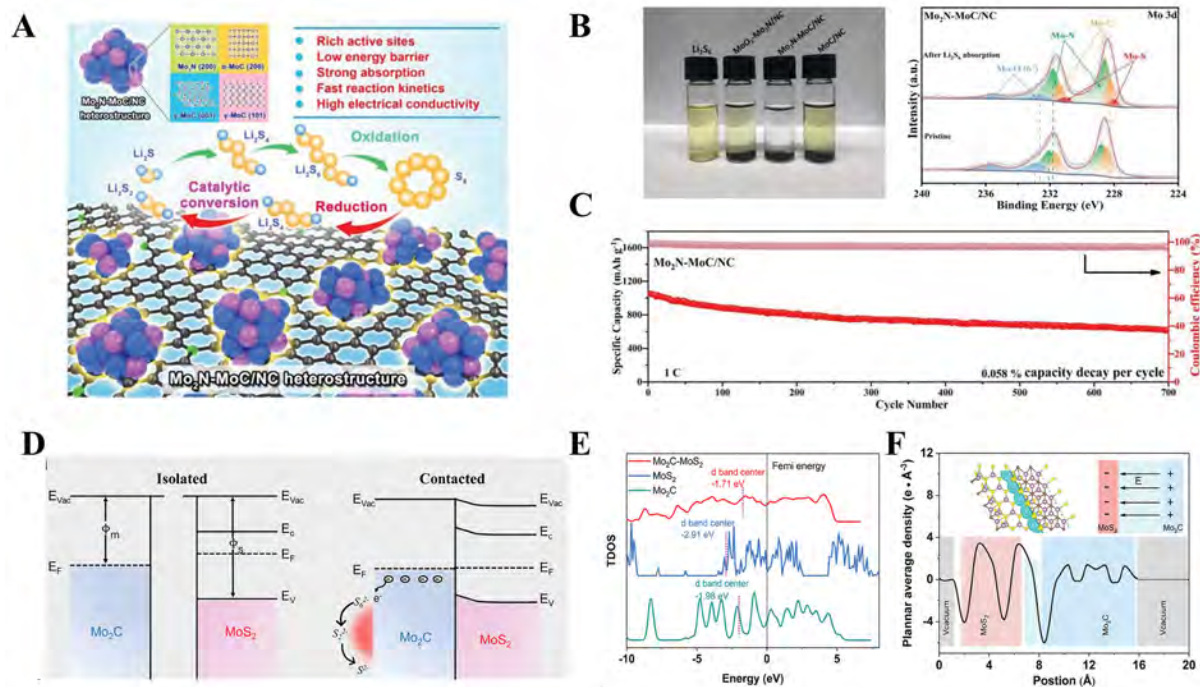


**Figure 10.**  $\text{MoC}_x/\text{MoN}_x$  heterostructures for LSBs. (A) Schematic illustration for the efficient trapping-diffusion-conversion of soluble LiPSs to solid  $\text{Li}_2\text{S}$  on the  $\text{Mo}_2\text{N-MoC/NC-PP}$ . (B) Photograph of the  $\text{Li}_2\text{S}_6$  adsorption tests and High-resolution XPS spectra before and after  $\text{Li}_2\text{S}_6$  adsorption tests. (C) Long-term cycling performance of the battery with  $\text{Mo}_2\text{N-MoC/NC-PP}$  at 1 C. Reproduced with permission from Ref. [96] Copyright 2023, Wiley-VCH. (D) Energy bands between  $\text{Mo}_2\text{C}$  and  $\text{MoS}_2$  before and after the Schottky contact. (E) TDOS for  $\text{Mo}_2\text{C-MoS}_2$ , MXene  $\text{Mo}_2\text{C}$  and  $\text{MoS}_2$  models. (F) Charge density difference for  $\text{Mo}_2\text{C-MoS}_2$  in-plane multi-heterostructures. (Insets) The ball-and-stick model of  $\text{Mo}_2\text{C-MoS}_2$  (left) and the illustration of the built-in electric fields (right). Reproduced with permission from Ref. [100] Copyright 2024, Wiley-VCH.

$\text{MoS}_2$  in-plane multi-heterostructures by the topological conversion of sandwich-like mesoporous  $\text{Mo}_2\text{C-SiO}_2$  layers in sulfur vapor, followed by the removal of  $\text{SiO}_2$  [100]. During the conversion, the exposed  $\text{Mo}_2\text{C}$  is transformed into the 2H phase  $\text{MoS}_2$ , while the covered  $\text{Mo}_2\text{C}$  remains stable, resulting in a layer that combines metallic  $\text{Mo}_2\text{C}$  MXene and semiconducting  $\text{MoS}_2$  [Figure 10D]. The  $\text{Mo}_2\text{C-MoS}_2$  layer with multiple heterointerfaces, built-in electric fields, and abundant defects improves the electrochemically active surface area ( $16.4 \text{ mF cm}^{-2}$ ) [Figure 10E and F]. This structure not only facilitates the bidirectional sulfur electrochemistry between solid  $\text{Li}_2\text{S}$  and soluble LiPSs but also enhances the transfer kinetics of electrons and ions, resulting in a high rate of  $642 \text{ mAh g}^{-1}$  at 5 C and long-term cycle lifetime (1,000 cycles at 5 C) in Li-S batteries.

Du *et al.* proposed a novel heterogeneous catalysis/deposition mechanism to enhance polysulfide conversion [101]. A heterostructured  $\text{Mo}_2\text{C}/\alpha\text{-MoO}_3/\text{G}$  nanomaterial was synthesized, featuring crystalline and amorphous phases with electronic delocalization and a built-in electric field. These features boost polysulfide conversion kinetics by increasing reaction rates and lowering activation energies. They also optimize  $\text{Li}_2\text{S}$  deposition, yielding a uniform 3D progressive nucleation (3DP) morphology and rapid  $\text{Li}^+$  diffusion on the catalyst surface. Consequently, even under a lean electrolyte level of  $9.3 \mu\text{L mg}^{-1}$ , the LSB with  $\text{Mo}_2\text{C}/\alpha\text{-MoO}_3/\text{G}$  delivers an initial specific capacity of  $1,055 \text{ mAh g}^{-1}$  and an areal capacity of  $4 \text{ mAh cm}^{-2}$ .

Heterostructures integrate distinct domains with differing properties, achieving synergistic effects through interfacial interactions that exceed simple component mixtures. Their catalytic mechanisms include (1) adsorption-catalysis synergy; (2) tandem catalysis; (3) bidirectional reaction promotion; and (4) electronic structure modulation<sup>[102]</sup>. Therefore, heterostructures composed of TMCs with different Fermi levels can induce interfacial built-in electric fields and electron transfer, triggering electron redistribution and localized atomic rearrangement. This modulates electronic structures (e.g., band structure, d/p-band centers, electron occupancy, and valence states), significantly enhancing adsorption catalysis, thus suppressing polysulfide shuttling and improving rate/cycling performance<sup>[103]</sup>.

## CONCLUSION AND PROSPECTS

In summary, Li-S batteries have emerged as promising candidates for next-generation ESSs because of advantages such as high theoretical energy density, cost-effectiveness, and environmental compatibility. However, their practical application is hindered by intrinsic challenges, including the shuttle effect of LiPSs (LiPSs), sluggish redox kinetics, and the instability of the lithium metal anode. To overcome these obstacles, Mo-based carbides ( $\text{MoC}_x$ ) and nitrides ( $\text{MoN}_x$ ) have demonstrated exceptional potential as electrocatalysts and structural components due to their unique electronic structure, superior catalytic activity, and high electrical conductivity. The integration of  $\text{MoC}_x$  and  $\text{MoN}_x$  into Li-S battery systems, as cathode hosts, separator modifications, or multifunctional interlayers, has shown significant promise in mitigating the shuttle effect, accelerating LiPSs conversion, and improving sulfur utilization.

Notably, nanostructured Mo-based materials such as  $\text{Mo}_2\text{C}$  and  $\text{MoN}$  and their heterostructures exhibit tunable electronic properties, strong adsorption of LiPSs, and excellent catalytic activity. These materials facilitate rapid polysulfide conversion and uniform lithium deposition, resulting in improved cycling stability and rate performance. Heterostructure engineering, such as combining  $\text{MoC}_x$  and  $\text{MoN}_x$  or integrating them with carbon frameworks and metallic compounds, increases active site exposure, creates built-in electric fields, and optimizes electron/ion transfer kinetics. These advancements have spurred significant breakthroughs, including high capacities, low-capacity fade rates, and excellent long-term cycling stability under high sulfur loadings and lean electrolyte conditions.

**Table 1** summarizes the applications of Mo-based compounds with different nonmetallic elements in Li-S batteries. Mo-based materials exhibit diverse chemical compositions and morphological structures, and variations in nonmetallic elements significantly influence their adsorption capacity and catalytic activity toward LiPSs. The modulation of anions alters the  $\Delta d-p$  (representing the p-d hybridization state between Mo and nonmetallic elements), thereby regulating the LiPSs conversion pathways and enhancing reaction kinetics<sup>[112-114]</sup>. Consequently,  $\Delta d-p$  serves as a more accurate descriptor than the d-band center for evaluating the electrocatalytic performance of materials, as it fundamentally governs the catalytic mechanism. When the active Mo sites in Mo-based compounds interact with  $\text{Li}_2\text{S}_4$ , electrons transfer from  $\text{Li}_2\text{S}_4$  molecules to the catalyst. The  $\Delta d-p$  of the catalyst determines the redistribution of electrons within the compound after thermodynamic adsorption, which in turn dictates catalytic performance. Specifically, catalysts with smaller  $\Delta d-p$  exhibit lower energy barriers for redistributing additional electrons in the system, leading to stronger interactions with  $\text{Li}_2\text{S}_4$ . This is because the magnitude of  $\Delta d-p$  governs electron transfer during  $\text{Li}_2\text{S}_4$  conversion: 1. Catalysts with smaller  $\Delta d-p$  facilitate electron transfer to nonmetallic elements in the compound, increasing the total electron transfer during interactions with  $\text{Li}_2\text{S}_4$ ; and 2. This process lowers the energy level of the antibonding orbitals in S-S bonds, thereby reducing the activation energy for electrochemical catalysis and improving reaction kinetics.

**Table 1. The applications of transition metal compound materials in Li-S batteries**

Classification	Material	Structure characteristics	Sulfur loading (mg/cm <sup>2</sup> )/(%)	Cycle number (rate)	Initial/final capacity (mAh/g)	Refs.
Molybdenum carbides	Mo <sub>2</sub> C/C	Nanoparticles	1.5 /N/A	400 (1 C)	798/612	[60]
	Mo <sub>2</sub> C/NG	Quantum dots	1.5 /N/A	100 (0.2 C)	1,230/1,146	[68]
	α-MoC <sub>1-x</sub> /NC	Nanocrystallites	4.3	85 (0.1 C)	845/785	[71]
Molybdenum nitrides	Mo <sub>2</sub> N/C	Porous	N/A/N/A	100 (0.5 C)	995/914	[75]
	Mo <sub>2</sub> N/NG/PP	Quantum dots	N/A	300 (0.5 C)	858/706	[76]
	MoN/CMK-5	Bimodal pore structure	N/A/N/A	1,000 (5 C)	475/344	[79]
	Co/MoN	Nanoparticle	1.2/N/A	500 (1 C)	860/554	[83]
Other molybdenum-based compounds	MoS <sub>2</sub> /CNT/S	Cross-stacked membrane	2.6/N/A	50 (0.2 C)	855/495	[104]
	MoO <sub>3</sub> /CNF	Nanofiber membrane	N/A,N/A	500 (0.2 C)	776/427	[105]
	CMoP/CMK/3	Clusters confined into mesoporous carbon	N/A/70%	500 (2 C)	902/811	[106]
	CoO/MoO <sub>3</sub> @NC	Hollow structure	1.2/ N/A	100 (0.1 C)	1,256.8/802.8	[107]
	Mo <sub>1-x</sub> Nb <sub>x</sub> S <sub>2</sub> HNTs	Nanosheets assembled hollow nanotubes	3.13/N/A	47 (0.5 C)	613/434	[108]
Other transition metal compounds	Fe <sub>3</sub> O <sub>4</sub> @GCF	Nanoparticle	1.5/N/A	100 (1 C)	1,245/700	[109]
	Fe <sub>2</sub> O <sub>3</sub> /N-MC	Nanocrystalline structure	5.1/72.5	500 (1 C)	19.4/3.69 (mAh/cm <sup>2</sup> )	[110]
	CoSe@NC	Nanofiber membrane	1.2-1.5/69.19	200 (1 C)	797/669.1	[111]
	VN/C@TCF	Triple-nanolayers	1.5/N/A	500 (1 C)	978.1/661.2	[112]

Despite these achievements, challenges remain that must be addressed to enable the large-scale commercialization of Li-S batteries. Key limitations include: 1. Material and Cost Constraints: Molybdenum concentrate (MoS<sub>2</sub>) trades at ~20-25 USD/lb, while MoN<sub>x</sub>/MoC<sub>x</sub> synthesis requires additional nitridation/carbonization steps, increasing costs by 30%-50%; and 2. Scalability Barriers: Energy-intensive synthesis methods [e.g., high-temperature processing, chemical vapor deposition (CVD), sol-gel] hinder scalable production of MoC<sub>x</sub>/MoN<sub>x</sub> due to specialized equipment demands

First, the scalability and cost-effectiveness of Mo-based materials with precise nanostructures and heterostructures must be improved. The development of eco-friendly and economically viable synthesis methods, such as utilizing bio-based carbon sources or scalable templating approaches, will be essential. Secondly, the long-term stability of Mo-based catalysts under operating conditions, including their resistance to external factors and sulfur poisoning, requires further investigation. Doping strategies and surface engineering can be employed to enhance the durability of these materials. Thirdly, the interaction mechanisms between Mo-based materials and LiPSs must be better understood by performing advanced theoretical calculations and *in situ* characterization in order to gain insights into the optimization of the catalytic activity and adsorption capabilities.

Looking ahead, future research should focus on the design of multifunctional Mo-based composites by combining the catalytic benefits of  $\text{MoC}_x$  and  $\text{MoN}_x$  with the stability and conductivity of carbon architectures or other metallic compounds. Additionally, novel heterostructures, such as Mo-based materials integrated with transition metal sulfides, oxides, or selenides, may unfold new synergies. Finally, practical considerations, such as enhanced sulfur loadings, reduced electrolyte amount, and improved safety through dendrite-free lithium deposition<sup>[115]</sup>, must be prioritized to bridge the gap between laboratory demonstrations and real-world applications.

On the other hand, replacing liquid electrolytes with solid-state electrolytes (SSEs), particularly sulfide-based SSEs in all-solid-state Li-S batteries (ASSLSBs), can physically eliminate polysulfide shuttle while mitigating safety risks associated with volatile and flammable solvents in conventional liquid electrolyte batteries<sup>[116]</sup>. However, the sulfur cathodes in ASSLSBs suffer from slow reaction kinetics and insufficient conductivity, necessitating the incorporation of substantial carbon additives and SSEs to enhance ionic/electronic transport around sulfur. Nevertheless, the resulting high interfacial contact area between SSEs and carbon induces non-negligible oxidative decomposition of SSEs during battery charging. Mo-based compounds demonstrate exceptional interfacial compatibility and stability with sulfides, serving as alternative sulfur hosts to effectively mitigate this issue<sup>[117,118]</sup>. Therefore, the application of  $\text{MoC}_x/\text{MoN}_x$  in ASSLSBs can become one of the research hotspots and challenges in the future LSB field.

By addressing these challenges and leveraging the unique properties of Mo-based materials, Li-S batteries can achieve the breakthroughs needed to become a competitive and sustainable solution for large-scale energy storage. The continued innovation in materials design, coupled with a deeper understanding of the underlying mechanisms, holds the potential to revolutionize the field of energy storage and significantly advance the transition to a green economy with carbon neutrality.

## DECLARATIONS

### Authors' contributions

Framework design and manuscript writing: Fan, Q.

Manuscript review: Song, H.; Gao, B.; Wang, L.; Chu, P. K.

Administrative support, funding acquisition and supervision: Wang, L.; Chu, P. K.; Huo, K.

### Availability of data and materials

Not applicable.

### Financial support and sponsorship

This work was supported by the National Natural Science Foundation of China (Grant No. 22308109), Guangdong Basic and Applied Basic Research Foundation (Grant No. 2024A1515010678), Basic and Applied Basic Research Project of Guangzhou (Grant No. SL2023A04J00635), and City University of Hong Kong Donation Research Grants (DON-RMG 9229021 and 9229061).

### Conflicts of interest

All authors declared that there are no conflicts of interest.

### Ethical approval and consent to participate

Not applicable.

## Consent for publication

Not applicable.

## Copyright

© The Author(s) 2025.

## REFERENCES

1. Khan, F. M. N. U.; Rasul, M. G.; Sayem, A.; Mandal, N. K. Design and optimization of lithium-ion battery as an efficient energy storage device for electric vehicles: a comprehensive review. *J. Energy. Storage.* **2023**, *71*, 108033. DOI
2. Cheng, W.; Zhao, M.; Lai, Y.; et al. Recent advances in battery characterization using in situ XAFS, SAXS, XRD, and their combining techniques: from single scale to multiscale structure detection. *Exploration* **2024**, *4*, 20230056. DOI PubMed PMC
3. Nekahi, A.; Madikere, R. R. A. K.; Li, X.; Deng, S.; Zaghbi, K. Rechargeable batteries for the electrification of society: past, present, and future. *Electrochem. Energy. Rev.* **2025**, *8*, 235. DOI
4. Park, C. Y.; Kim, J.; Lim, W. G.; Lee, J. Toward maximum energy density enabled by anode-free lithium metal batteries: recent progress and perspective. *Exploration* **2024**, *4*, 20210255. DOI PubMed PMC
5. Huang, Z.; Jaumaux, P.; Sun, B.; et al. High-energy room-temperature sodium-sulfur and sodium-selenium batteries for sustainable energy storage. *Electrochem. Energy. Rev.* **2023**, *6*, 182. DOI
6. Guo, Y.; Niu, Q.; Pei, F.; et al. Interface engineering toward stable lithium-sulfur batteries. *Energy. Environ. Sci.* **2024**, *17*, 1330-67. DOI
7. Sharma, R.; Kumar, H.; Kumar, G.; et al. Progress and challenges in electrochemical energy storage devices: Fabrication, electrode material, and economic aspects. *Chem. Eng. J.* **2023**, *468*, 143706. DOI
8. Liu, R.; Wei, Z.; Peng, L.; et al. Establishing reaction networks in the 16-electron sulfur reduction reaction. *Nature* **2024**, *626*, 98-104. DOI
9. Wu, J.; Ye, T.; Wang, Y.; et al. Understanding the catalytic kinetics of polysulfide redox reactions on transition metal compounds in Li-S batteries. *ACS. Nano.* **2022**, *16*, 15734-59. DOI
10. Li, J.; Niu, Z.; Guo, C.; Li, M.; Bao, W. Catalyzing the polysulfide conversion for promoting lithium sulfur battery performances: a review. *J. Energy. Chem.* **2021**, *54*, 434-51. DOI
11. Li, G.; Wang, S.; Zhang, Y.; Li, M.; Chen, Z.; Lu, J. Revisiting the role of polysulfides in lithium-sulfur batteries. *Adv. Mater.* **2018**, *30*, e1705590. DOI
12. Yu, J.; Pinto-Huguet, I.; Zhang, C. Y.; et al. Mechanistic insights and technical challenges in sulfur-based batteries: a comprehensive in situ/operando monitoring toolbox. *ACS. Energy. Lett.* **2024**, *9*, 6178-214. DOI PubMed PMC
13. Zhou, L.; Danilov, D. L.; Qiao, F.; et al. Sulfur reduction reaction in lithium-sulfur batteries: mechanisms, catalysts, and characterization. *Adv. Energy. Mater.* **2022**, *12*, 2202094. DOI
14. Deng, R.; Wang, M.; Yu, H.; et al. Recent advances and applications toward emerging lithium-sulfur batteries: working principles and opportunities. *Energy. Environ. Mater.* **2022**, *5*, 777-99. DOI
15. Yu, S.; Cai, W.; Chen, L.; Song, L.; Song, Y. Recent advances of metal phosphides for Li-S chemistry. *J. Energy. Chem.* **2021**, *55*, 533-48. DOI
16. Hencz, L.; Chen, H.; Wu, Z.; et al. Highly branched amylopectin binder for sulfur cathodes with enhanced performance and longevity. *Exploration* **2022**, *2*, 20210131. DOI PubMed PMC
17. Zhai, P.; Peng, H.; Cheng, X.; et al. Scaled-up fabrication of porous-graphene-modified separators for high-capacity lithium-sulfur batteries. *Energy. Storage. Mater.* **2017**, *7*, 56-63. DOI
18. Zhou, G.; Li, L.; Ma, C.; et al. A graphene foam electrode with high sulfur loading for flexible and high energy Li-S batteries. *Nano. Energy.* **2015**, *11*, 356-65. DOI
19. He, G.; Evers, S.; Liang, X.; Cuisinier, M.; Garsuch, A.; Nazar, L. F. Tailoring porosity in carbon nanospheres for lithium-sulfur battery cathodes. *ACS. Nano.* **2013**, *7*, 10920-30. DOI PubMed
20. Ruan, J.; Sun, H.; Song, Y.; et al. Constructing 1D/2D interwoven carbonous matrix to enable high-efficiency sulfur immobilization in Li-S battery. *Energy. Mater.* **2022**, *1*, 100018. DOI
21. Wang, Q.; Zhao, H.; Li, B.; et al. MOF-derived Co<sub>9</sub>S<sub>8</sub> nano-flower cluster array modified separator towards superior lithium sulfur battery. *Chin. Chem. Lett.* **2021**, *32*, 1157-60. DOI
22. Tao, X.; Wang, J.; Liu, C.; et al. Balancing surface adsorption and diffusion of lithium-polysulfides on nonconductive oxides for lithium-sulfur battery design. *Nat. Commun.* **2016**, *7*, 11203. DOI PubMed PMC
23. He, J.; Chen, Y.; Manthiram, A. Vertical Co<sub>9</sub>S<sub>8</sub> hollow nanowall arrays grown on a Celgard separator as a multifunctional polysulfide barrier for high-performance Li-S batteries. *Energy. Environ. Sci.* **2018**, *11*, 2560-8. DOI
24. Liu, D.; Zhang, C.; Zhou, G.; et al. Catalytic effects in lithium-sulfur batteries: promoted sulfur transformation and reduced shuttle effect. *Adv. Sci.* **2018**, *5*, 1700270. DOI PubMed PMC
25. Zheng, Y.; Yi, Y.; Fan, M.; et al. A high-entropy metal oxide as chemical anchor of polysulfide for lithium-sulfur batteries. *Energy. Storage. Mater.* **2019**, *23*, 678-83. DOI

26. Liu, X.; Huang, J. Q.; Zhang, Q.; Mai, L. Nanostructured metal oxides and sulfides for lithium-sulfur batteries. *Adv. Mater.* **2017**, *29*, 1601759. DOI
27. Ye, X.; Wu, F.; Xue, Z.; et al. Accelerated polysulfide conversion by rationally designed NiS<sub>2</sub>-CoS<sub>2</sub> heterostructure in lithium-sulfur batteries. *Adv. Funct. Mater.* **2025**, *35*, 2417776. DOI
28. Huang, C.; Yu, J.; Zhang, C. Y.; et al. Electronic spin alignment within homologous NiS<sub>2</sub>/NiSe<sub>2</sub> heterostructures to promote sulfur redox kinetics in lithium-sulfur batteries. *Adv. Mater.* **2024**, *36*, e2400810. DOI
29. Zhao, H.; Wu, J.; Chen, T.; et al. Cobalt-doped molybdenum sulfide as an interlayer facilitates polysulfide conversion to obtain high-performance lithium-sulfur batteries. *J. Energy Storage*. **2024**, *101*, 113903. DOI
30. Ren, X.; Wu, H.; Guo, Y.; et al. The impact of oxygen content in O-doped MoS<sub>2</sub> on the kinetics of polysulfide conversion in Li-S batteries. *Small* **2024**, *20*, e2312256. DOI
31. Li, R.; Sun, H.; Chang, C.; Yao, Y.; Pu, X.; Mai, W. In situ induced cation-vacancies in metal sulfides as dynamic electrocatalyst accelerating polysulfides conversion for Li-S battery. *J. Energy Chem.* **2022**, *75*, 74-82. DOI
32. Yao, Y.; Chang, C.; Sun, H.; et al. Hollow Ni<sub>3</sub>Se<sub>4</sub> with high tap density as a carbon-free sulfur immobilizer to realize high volumetric and gravimetric capacity for lithium-sulfur batteries. *ACS Appl. Mater. Interfaces*. **2022**, *14*, 25267-77. DOI
33. Cai, D.; Liu, B.; Zhu, D.; et al. Ultrafine Co<sub>3</sub>Se<sub>4</sub> nanoparticles in nitrogen-doped 3D carbon matrix for high-stable and long-cycle-life lithium-sulfur batteries. *Adv. Energy Mater.* **2020**, *10*, 1904273.
34. Mosavati, N.; Salley, S. O.; Ng, K. S. Characterization and electrochemical activities of nanostructured transition metal nitrides as cathode materials for lithium sulfur batteries. *J. Power. Sources*. **2017**, *340*, 210-6. DOI
35. Jeong, T.; Choi, D. S.; Song, H.; et al. Heterogeneous catalysis for lithium-sulfur batteries: enhanced rate performance by promoting polysulfide fragmentations. *ACS Energy Lett.* **2017**, *2*, 327-33. DOI
36. Zhang, L.; Chen, X.; Wan, F.; et al. Enhanced electrochemical kinetics and polysulfide traps of indium nitride for highly stable lithium-sulfur batteries. *ACS Nano*. **2018**, *12*, 9578-86. DOI
37. Weng, W.; Xiao, J.; Shen, Y.; Liang, X.; Lv, T.; Xiao, W. Molten salt electrochemical modulation of iron-carbon-nitrogen for lithium-sulfur batteries. *Angew. Chem. Int. Ed.* **2021**, *60*, 24905-9. DOI
38. Wang, S.; Liu, X.; Duan, H.; Deng, Y.; Chen, G. Fe<sub>3</sub>C/Fe nanoparticles embedded in N-doped porous carbon nanosheets and graphene: a thin functional interlayer for PP separator to boost performance of Li-S batteries. *Chem. Eng. J.* **2021**, *415*, 129001. DOI
39. Ye, Z.; Jiang, Y.; Qian, J.; et al. Exceptional adsorption and catalysis effects of hollow polyhedra/carbon nanotube confined CoP nanoparticles superstructures for enhanced lithium-sulfur batteries. *Nano. Energy*. **2019**, *64*, 103965. DOI
40. Wu, Z.; Chen, S.; Wang, L.; et al. Implanting nickel and cobalt phosphide into well-defined carbon nanocages: a synergistic adsorption-electrocatalysis separator mediator for durable high-power Li-S batteries. *Energy Storage Mater.* **2021**, *38*, 381-8. DOI
41. Wang, F.; Han, Y.; Xu, R.; et al. Establishing transition metal phosphides as effective sulfur hosts in lithium-sulfur batteries through the triple effect of "confinement-adsorption-catalysis". *Small* **2023**, *19*, e2303599. DOI
42. Susarla, S.; Puthirath, A. B.; Tsafack, T.; Salpekar, D.; Babu, G.; Ajayan, P. M. Atomic-level alloying of sulfur and selenium for advanced lithium batteries. *ACS Appl. Mater. Interfaces*. **2020**, *12*, 1005-13. DOI PubMed
43. Liu, Q.; Wu, Y.; Li, D.; et al. Dilute alloying to implant activation centers in nitride electrocatalysts for lithium-sulfur batteries. *Adv. Mater.* **2023**, *35*, e2209233. DOI
44. Zhao, M.; Li, B. Q.; Peng, H. J.; Yuan, H.; Wei, J. Y.; Huang, J. Q. Lithium-sulfur batteries under lean electrolyte conditions: challenges and opportunities. *Angew. Chem. Int. Ed.* **2020**, *59*, 12636-52. DOI
45. Xie, J.; Li, B. Q.; Peng, H. J.; et al. Implanting atomic cobalt within mesoporous carbon toward highly stable lithium-sulfur batteries. *Adv. Mater.* **2019**, *31*, e1903813. DOI
46. Li, B.; Kong, L.; Zhao, C.; et al. Expediting redox kinetics of sulfur species by atomic-scale electrocatalysts in lithium-sulfur batteries. *InfoMat* **2019**, *1*, 533-41. DOI
47. Zhang, Y.; Zhang, R.; Guo, Y.; Li, Y.; Li, K. A review on MoS<sub>2</sub> structure, preparation, energy storage applications and challenges. *J. Alloys. Compd.* **2024**, *998*, 174916. DOI
48. Cao, Y.; Lin, Y.; Wu, J.; et al. Two-dimensional MoS<sub>2</sub> for Li-S batteries: structural design and electronic modulation. *ChemSusChem* **2020**, *13*, 1392-408. DOI
49. Liu, Y.; Lin, Z.; Bettels, F.; et al. Molybdenum-based catalytic materials for Li-S batteries: strategies, mechanisms, and prospects. *Adv. Energy Sustain. Res.* **2023**, *4*, 2200145. DOI
50. Liu, Y.; Cui, C.; Liu, Y.; Liu, W.; Wei, J. Application of MoS<sub>2</sub> in the cathode of lithium sulfur batteries. *RSC Adv.* **2020**, *10*, 7384-95. DOI PubMed PMC
51. Hussain, I.; Amara, U.; Bibi, F.; et al. Mo-based MXenes: synthesis, properties, and applications. *Adv. Colloid. Interface. Sci.* **2024**, *324*, 103077. DOI
52. Hua, W.; Sun, H.; Xu, F.; Wang, J. A review and perspective on molybdenum-based electrocatalysts for hydrogen evolution reaction. *Rare Met.* **2020**, *39*, 335-51. DOI
53. Miao, M.; Pan, J.; He, T.; Yan, Y.; Xia, B. Y.; Wang, X. Molybdenum carbide-based electrocatalysts for hydrogen evolution reaction. *Chem. A. Eur. J.* **2017**, *23*, 10947-61. DOI
54. Wan, C.; Regmi, Y. N.; Leonard, B. M. Multiple phases of molybdenum carbide as electrocatalysts for the hydrogen evolution reaction. *Angew. Chem. Int. Ed.* **2014**, *53*, 6407-10. DOI PubMed
55. Ramqvist, L.; Hamrin, K.; Johansson, G.; Fahlman, A.; Nordling, C. Charge transfer in transition metal carbides and related

- compounds studied by ESCA. *J. Phys. Chem. Solids.* **1969**, *30*, 1835-47. DOI
56. Jansen, S. A.; Hoffmann, R. Surface chemistry of transition metal carbides: a theoretical analysis. *Surf. Sci.* **1988**, *197*, 474-508. DOI
57. Zhang, Y.; Wang, Y.; Guo, C.; Wang, Y. Molybdenum carbide-based photocatalysts: synthesis, functionalization, and applications. *Langmuir* **2022**, *38*, 12739-56. DOI
58. Zhong, Y.; Xia, X.; Shi, F.; Zhan, J.; Tu, J.; Fan, H. J. Transition metal carbides and nitrides in energy storage and conversion. *Adv. Sci.* **2016**, *3*, 1500286. DOI PubMed PMC
59. Xie, J.; Li, S.; Zhang, X.; et al. Atomically-thin molybdenum nitride nanosheets with exposed active surface sites for efficient hydrogen evolution. *Chem. Sci.* **2014**, *5*, 4615-20. DOI
60. Sun, M.; Wang, Z.; Li, X.; et al. Rational understanding of the catalytic mechanism of molybdenum carbide in polysulfide conversion in lithium-sulfur batteries. *J. Mater. Chem. A.* **2020**, *8*, 11818-23. DOI
61. Razaq, R.; Sun, D.; Xin, Y.; et al. Enhanced kinetics of polysulfide redox reactions on Mo<sub>2</sub>C/CNT in lithium-sulfur batteries. *Nanotechnology* **2018**, *29*, 295401. DOI
62. Qian, J.; Xing, Y.; Yang, Y.; et al. Enhanced electrochemical kinetics with highly dispersed conductive and electrocatalytic mediators for lithium-sulfur batteries. *Adv. Mater.* **2021**, *33*, e2100810. DOI
63. Wang, L.; He, L.; Cheng, Y.; et al. P-doped Mo<sub>2</sub>C nanoparticles embedded on carbon nanofibers as an efficient electrocatalyst for Li-S batteries. *Chem. Eng. J.* **2024**, *490*, 151530. DOI
64. Chen, K.; Zhu, Y.; Huang, Z.; et al. Strengthened d-p orbital hybridization on metastable cubic Mo<sub>2</sub>C for highly stable lithium-sulfur batteries. *ACS. Nano.* **2024**, *18*, 34791-802. DOI
65. Li, J.; Shi, K.; Pan, J.; et al. Designing electrochemical nanoreactors to accelerate Li<sub>2</sub>S<sub>1/2</sub> three-dimensional growth process and generating more Li<sub>2</sub>S for advanced Li-S batteries. *Renewables* **2023**, *1*, 341-52. DOI
66. Yang, J.; Zhao, S.; Lu, Y.; Zeng, X.; Lv, W.; Cao, G. In-situ topochemical nitridation derivative MoO<sub>2</sub>-Mo<sub>2</sub>N binary nanobelts as multifunctional interlayer for fast-kinetic Li-Sulfur batteries. *Nano. Energy.* **2020**, *68*, 104356. DOI
67. Ma, Y.; Chang, L.; Yi, D.; et al. Synergetic effect of block and catalysis on polysulfides by functionalized bilayer modification on the separator for lithium-sulfur batteries. *Energy. Mater.* **2024**, *4*, 400059. DOI
68. Yu, B.; Chen, D.; Wang, Z.; et al. Mo<sub>2</sub>C quantum dots@graphene functionalized separator toward high-current-density lithium metal anodes for ultrastable Li-S batteries. *Chem. Eng. J.* **2020**, *399*, 125837. DOI
69. Shi, H.; Sun, Z.; Lv, W.; et al. Necklace-like MoC sulfiphilic sites embedded in interconnected carbon networks for Li-S batteries with high sulfur loading. *J. Mater. Chem. A.* **2019**, *7*, 11298-304. DOI
70. Ji, Y.; Zhang, J.; Yang, N.; et al. MoC nanoparticles decorated carbon nanofibers loaded with Li<sub>2</sub>S as high-performance lithium sulfur battery cathodes. *Appl. Surf. Sci.* **2025**, *679*, 161263. DOI
71. Li, H.; Zheng, W.; Wu, H.; Fang, Y.; Li, L.; Yuan, W. Ultra-dispersed  $\alpha$ -MoC<sub>1-x</sub> embedded in a plum-like N-doped carbon framework as a synergistic adsorption-electrocatalysis interlayer for high-performance Li-S batteries. *Small* **2024**, *20*, e2306140. DOI
72. Zhang, H.; Jin, H.; Yang, Y.; et al. Understanding the synergetic interaction within  $\alpha$ -MoC/ $\beta$ -Mo<sub>2</sub>C heterostructured electrocatalyst. *J. Energy. Chem.* **2019**, *35*, 66-70. DOI
73. Han, K.; Guo, D.; Li, M.; et al. Mixed valence Mo<sub>2</sub>C-MoC/C catalyst enhances polysulfides conversion kinetics in lithium-sulfur batteries. *Appl. Surf. Sci.* **2024**, *663*, 160138. DOI
74. Liu, X.; Wang, J.; Wang, W.; et al. Interfacial synergy in Mo<sub>2</sub>C/MoC heterostructure promoting sequential polysulfide conversion in high-performance lithium-sulfur battery. *Small* **2024**, *20*, e2307902. DOI
75. Jiang, G.; Xu, F.; Yang, S.; Wu, J.; Wei, B.; Wang, H. Mesoporous, conductive molybdenum nitride as efficient sulfur hosts for high-performance lithium-sulfur batteries. *J. Power. Sources.* **2018**, *395*, 77-84. DOI
76. Ma, F.; Srinivas, K.; Zhang, X.; et al. Mo<sub>2</sub>N Quantum dots decorated N-doped graphene nanosheets as dual-functional interlayer for dendrite-free and shuttle-free lithium-sulfur batteries. *Adv. Funct. Mater.* **2022**, *32*, 2206113. DOI
77. Yang, M.; Liu, P.; Qu, Z.; et al. Nitrogen-vacancy-regulated Mo<sub>2</sub>N quantum dots electrocatalyst enables fast polysulfides redox for high-energy-density lithium-sulfur batteries. *Nano. Energy.* **2022**, *104*, 107922. DOI
78. Cheng, M.; Xing, Z.; Yan, R.; et al. Oxygen-modulated metal nitride clusters with moderate binding ability to insoluble Li<sub>2</sub>S<sub>x</sub> for reversible polysulfide electrocatalysis. *InfoMat* **2023**, *5*, e12387. DOI
79. Liu, Z.; Lian, R.; Wu, Z.; et al. Ordered dual-channel carbon embedded with molybdenum nitride catalytically induced high-performance lithium-sulfur battery. *Chem. Eng. J.* **2022**, *431*, 134163. DOI
80. Tan, T.; Chen, N.; Wang, Z.; et al. Thorn-like carbon nanofibers combined with molybdenum nitride nanosheets as a modified separator coating: an efficient chemical anchor and catalyst for Li-S batteries. *ACS. Appl. Energy. Mater.* **2022**, *5*, 6654-62. DOI
81. Li, R.; Peng, H.; Wu, Q.; et al. Sandwich-like catalyst-carbon-catalyst trilayer structure as a compact 2D host for highly stable lithium-sulfur batteries. *Angew. Chem. Int. Ed.* **2020**, *59*, 12129-38. DOI
82. Liu, Y.; Xu, J.; Cao, Y.; et al. Promoting polysulfide redox kinetics by tuning the non-metallic p-band of Mo-based compounds. *J. Mater. Chem. A.* **2022**, *10*, 11477-87. DOI
83. Kong, Y.; Wang, L.; Mamoor, M.; et al. Co/Mon invigorated bilateral kinetics modulation for advanced lithium-sulfur batteries. *Adv. Mater.* **2024**, *36*, e2310143. DOI
84. Dewangan, K.; Patil, S. S.; Joag, D. S.; More, M. A.; Gajbhiye, N. S. Topotactical nitridation of  $\alpha$ -MoO<sub>3</sub> fibers to  $\gamma$ -Mo<sub>2</sub>N fibers and its field emission properties. *J. Phys. Chem. C.* **2010**, *114*, 14710-5. DOI

85. Machon, D.; Daisenberger, D.; Soignard, E.; et al. High pressure - high temperature studies and reactivity of  $\gamma$ -Mo<sub>2</sub>N and  $\delta$ -MoN. *Phys. Status Solidi*. **2006**, *203*, 831-6. DOI
86. Liu, S.; Xiao, J.; Lu, X. F.; Wang, J.; Wang, X.; Lou, X. W. D. Efficient electrochemical reduction of CO<sub>2</sub> to HCOOH over Sub-2 nm SnO<sub>2</sub> quantum wires with exposed grain boundaries. *Angew. Chem. Int. Ed.* **2019**, *58*, 8499-503. DOI
87. Wang, C.; Wang, S.; He, Y.; et al. Combining fast Li-ion battery cycling with large volumetric energy density: grain boundary induced high electronic and ionic conductivity in Li<sub>4</sub>Ti<sub>5</sub>O<sub>12</sub> spheres of densely packed nanocrystallites. *Chem. Mater.* **2015**, *27*, 5647-56. DOI
88. Yang, J.; Cai, D.; Lin, Q.; et al. Regulating the Li<sub>2</sub>S deposition by grain boundaries in metal nitrides for stable lithium-sulfur batteries. *Nano. Energy*. **2022**, *91*, 106669. DOI
89. Niu, S.; Zhang, S.; Shi, R.; et al. Freestanding agaric-like molybdenum carbide/graphene/N-doped carbon foam as effective polysulfide anchor and catalyst for high performance lithium sulfur batteries. *Energy. Storage. Mater.* **2020**, *33*, 73-81. DOI
90. Wang, P.; Li, N.; Zhang, Z.; et al. Synergetic enhancement of polysulfide chemisorption and electrocatalysis over bicontinuous MoN@N-rich carbon porous nano-octahedra for Li-S batteries. *J. Mater. Chem. A*. **2019**, *7*, 21934-43. DOI
91. Chen, G.; Li, Y.; Zhong, W.; et al. MOFs-derived porous Mo<sub>2</sub>C-C nano-octahedrons enable high-performance lithium-sulfur batteries. *Energy. Storage. Mater.* **2020**, *25*, 547-54. DOI
92. Wang, Q.; Qin, B.; Jiang, Q.; et al. Highly dispersed conductive and electrocatalytic mediators enabling rapid polysulfides conversion for lithium sulfur batteries. *Chem. Eng. J.* **2023**, *476*, 146865. DOI
93. Huang, S.; Wang, Z.; Von, L. Y.; et al. Recent advances in heterostructure engineering for lithium-sulfur batteries. *Adv. Energy. Mater.* **2021**, *11*, 2003689. DOI
94. Lee, H.; Nam, H.; Moon, J. H. Seamless integration of nanoscale crystalline-amorphous MoO<sub>3</sub> domains for high-performance lithium-sulfur batteries. *Energy. Storage. Mater.* **2024**, *70*, 103551. DOI
95. Jiao, X.; Hu, J.; Zuo, Y.; Qi, J.; Yan, W.; Zhang, J. Self-recovery catalysts of ZnIn<sub>2</sub>S<sub>4</sub>@In<sub>2</sub>O<sub>3</sub> heterostructures with multiple catalytic centers for cascade catalysis in lithium-sulfur battery. *Nano. Energy*. **2024**, *119*, 109078. DOI
96. Zhao, M.; Tan, P.; Cai, D.; et al. Customizing component regulated dense heterointerfaces for crafting robust lithium-sulfur batteries. *Adv. Funct. Mater.* **2023**, *33*, 2211505. DOI
97. Zhang, W.; Li, H.; Tao, R.; et al. In-situ constructing hetero-structured Mo<sub>2</sub>C-Mo<sub>2</sub>N embedded in carbon nanosheet as an efficient separator modifier for high-performance lithium-sulfur batteries. *Chem. Eng. J.* **2023**, *475*, 146133. DOI
98. Li, X. H.; Antonietti, M. Metal nanoparticles at mesoporous N-doped carbons and carbon nitrides: functional Mott-Schottky heterojunctions for catalysis. *Chem. Soc. Rev.* **2013**, *42*, 6593-604. DOI PubMed
99. Wang, Y.; Zhang, R.; Sun, Z.; et al. Spontaneously formed mott-schottky electrocatalyst for lithium-sulfur batteries. *Adv. Mater. Inter.* **2020**, *7*, 1902092. DOI
100. Li, X.; Zuo, Y.; Zhang, Y.; et al. Controllable sulfurization of MXenes to in-plane multi-heterostructures for efficient sulfur redox kinetics. *Adv. Energy. Mater.* **2024**, *14*, 2303389. DOI
101. Du, S.; Yu, Y.; Liu, X.; et al. Heterostructure Mo<sub>2</sub>C/ $\alpha$ -MoO<sub>3</sub>/G catalyst based heterogeneous catalysis/deposition mechanism for high-performance Li-S battery. *Chem. Eng. J.* **2024**, *500*, 157002. DOI
102. Zhang, K.; Zhao, Z.; Chen, H.; et al. A review of advances in heterostructured catalysts for Li-S batteries: structural design and mechanism analysis. *Small* **2025**, *21*, e2409674. DOI
103. Chen, L.; Cao, G.; Li, Y.; et al. A review on engineering transition metal compound catalysts to accelerate the redox kinetics of sulfur cathodes for lithium-sulfur batteries. *Nanomicro. Lett.* **2024**, *16*, 97. DOI PubMed PMC
104. Yan, L.; Luo, N.; Kong, W.; et al. Enhanced performance of lithium-sulfur batteries with an ultrathin and lightweight MoS<sub>2</sub>/carbon nanotube interlayer. *J. Power. Sources*. **2018**, *389*, 169-77. DOI
105. Imtiaz, S.; Ali, Z. Z.; Razaq, R.; et al. Electrocatalysis on separator modified by molybdenum trioxide nanobelts for lithium-sulfur batteries. *Adv. Mater. Inter.* **2018**, *5*, 1800243. DOI
106. Wang, L.; Li, X.; Zhang, Y.; et al. Subnanometer MoP clusters confined in mesoporous carbon (CMK-3) as superior electrocatalytic sulfur hosts for high-performance lithium-sulfur batteries. *Chem. Eng. J.* **2022**, *446*, 137050. DOI
107. Jiang, Y.; Du, M.; Geng, P.; Sun, B.; Zhu, R.; Pang, H. CoO/MoO<sub>3</sub>@Nitrogen-doped carbon hollow heterostructures for efficient polysulfide immobilization and enhanced ion transport in lithium-sulfur batteries. *J. Colloid. Interface. Sci.* **2024**, *664*, 617-25. DOI PubMed
108. Song, M.; Liu, Y.; Wang, X.; et al. Atomic substitution engineering-induced domino synergistic catalysis in Li-S batteries. *Chem. Eng. J.* **2024**, *502*, 157926. DOI
109. Liu, Y.; Meng, Q.; Yang, R.; et al. Anchoring polysulfides with ternary Fe<sub>3</sub>O<sub>4</sub>/graphitic carbon/porous carbon fiber hierarchical structures for high-rate lithium-sulfur batteries. *J. Energy. Storage*. **2025**, *105*, 114591. DOI
110. Lu, Y.; Qin, J.; Shen, T.; et al. Hypercrosslinked polymerization enabled N-doped carbon confined Fe<sub>2</sub>O<sub>3</sub> facilitating Li polysulfides interface conversion for Li-S batteries. *Adv. Energy. Mater.* **2021**, *11*, 2101780. DOI
111. Jiang, X.; Zhang, S.; Zou, B.; et al. Electrospun CoSe@NC nanofiber membrane as an effective polysulfides adsorption-catalysis interlayer for Li-S batteries. *Chem. Eng. J.* **2022**, *430*, 131911. DOI
112. Liu, G.; Zeng, Q.; Sui, X.; et al. Modulating the d-p orbital coupling of manganese chalcogenides for efficient polysulfides conversion in lithium-sulfur batteries. *J. Power. Sources*. **2022**, *552*, 232244. DOI
113. Zhang, W.; Liu, J.; Cai, W.; et al. Engineering d-p orbital hybridization through regulation of interband energy separation for durable

- aqueous Zn//VO<sub>2</sub>(B) batteries. *Chem. Eng. J.* **2023**, 464, 142711. DOI
114. Yu, J.; Yong, X.; Lu, S. p-d orbital hybridization engineered single-atom catalyst for electrocatalytic ammonia synthesis. *Energy. Environ. Mater.* **2024**, 7, e12587. DOI
  115. Yu, Z.; Gan, C.; Mijailovic, A. S.; et al. Lithium dendrite deflection at mixed ionic-electronic conducting interlayers in solid electrolytes. *Adv. Energy Mater.* **2025**, 15, 2403179. DOI
  116. Shen, K.; Shi, W.; Song, H.; et al. Solid catholyte with regulated interphase redox for all-solid-state lithium-sulfur batteries. *Adv. Mater.* **2025**, 37, e2417171. DOI
  117. George, C.; Morris, A. J.; Modarres, M. H.; De, V. M. Structural evolution of electrochemically lithiated MoS<sub>2</sub> nanosheets and the role of carbon additive in Li-ion batteries. *Chem. Mater.* **2016**, 28, 7304-10. DOI PubMed PMC
  118. Li, H.; Wang, R.; Song, J.; et al. In situ-constructed Li<sub>x</sub>MoS<sub>2</sub> with highly exposed interface boosting high-loading and long-life cathode for all-solid-state Li-S batteries. *Energy. Environ. Mater.* **2024**, 7, e12687. DOI